



Technisch Naturwissenschaftliche  
Fakultät

# **Biological functionalization of organic semiconductor interface**

Masterarbeit

zur Erlangung des akademischen Grades

Diplom-Ingenieurin

im Masterstudium

Technische Chemie

Eingereicht von:

Halime Coskun, BSc.

Angefertigt am:

Linz Institute of Organic Solar Cells (LIOS)/Institute of Physical Chemistry

Beurteilung:

o. Univ. Prof. Mag. Dr. DDr. h.c. Niyazi Serdar Sariciftci

Mitwirkung:

Dr. Eric Daniel Głowacki, MSc.

Linz, Oktober 2015

# Eidesstattliche Erklärung

Ich erkläre an Eides statt, dass ich die vorliegende Masterarbeit selbstständig und ohne fremde Hilfe verfasst, andere als die angegebenen Quellen und Hilfsmittel nicht benutzt bzw. die wörtlich oder sinngemäß entnommenen Stellen als solche kenntlich gemacht habe. Die vorliegende Masterarbeit ist mit dem elektronisch übermittelten Textdokument identisch.

I hereby declare under oath that the submitted master thesis has been written solely by me without any outside assistance, information other than provided sources or aids have not been used and those used have been fully documented. The master thesis here present is identical to the electronically transmitted text document.

Linz, October 2015

.....

# Abstract

The field of bioelectronics concerns the interface of electronics with living systems. Organic electronics, by virtue of the chemical compatibility and functionality of organic materials, is a natural choice as an active material for this field. This newly developing field has begun to explore and realize innovative processes and living tissues, as well as a range of both in vitro and in vivo sensors and detectors.

Based on this motivation to develop bioelectronic devices and biosensors, the present master thesis deals with the biological surface functionalization of organic field-effect transistors (OFETs). The aim of this work is to develop organic field-effect transistors from a biocompatible, low-cost, stable and non-toxic semiconductor that can afford immediate operation in an aqueous biomolecular environment as specific and selective biosensors.

Recently in our group, hydrogen-bonded semiconductors have emerged as potential materials for bioelectronics based on their favourable electronic performance, promising operational stability, and the presence of chemical handles in the form of amine and carbonyl functional groups. The pigment material epindolidione (EPI) was explored in this work, and was found to indeed be a promising bioelectronics material.

Epindolidione was processed into semiconducting polycrystalline thin films by vacuum evaporation. Protocols for biofunctionalization of these surfaces were explored in detail for two model biological systems: The *Rhodobacter sphaeroides* photosynthetic reaction center (RC) and streptavidin. For the RC, a method for covalent biofunctionalization was developed using a suberic acid based linker (SUB). For streptavidin, a functionalized biotin (B7) ester was used as a linker. The bioconjugation reaction was verified using atomic force microscopy (AFM), water contact angle measurements, and Fourier-transform infrared spectroscopy (FTIR) on the surface-modified samples. Using this combination of methods, the surface functionalization protocol was optimized and the successful covalent modification of the surface was confirmed.

Knowing that the EPI films could be successfully modified, we then endeavoured to verify that both the protein and the semiconductor film retained their respective properties.

To this end, we fabricated organic field-effect transistors with EPI. We have found that these transistor devices remain operational in aqueous environments at harsh pH conditions from 3-10. So would it be possible to fabricate an epindolidione OFET, functionalize it on the device surface with aqueous linkers and proteins via simple processing and then finally detect those biomolecules? Would such a sensitive device survive these circumstances? To find answers to all these questions, bottom-gate/top-contact organic field-effect transistors made out of epindolidione were produced and operated in linear-mode at low-voltages in order to avoid any unexpected electrochemical reactions. Clear evidences for the appearance of the linkers on the semiconductor surface were obtained in transfer characteristics responses to different biomolecules.

In summary, it was shown in this work that the surface modification of the hydrogen-bonded organic semiconductor epindolidione was achieved by covalent bonding with various biomolecules. Hence, we believe that after a further design and development epindolidione can be used in different biosensing applications with new approaches. In the near future functionalization of epindolidione surface for interfacing with neurons for medical purposes is conceivable.

# Kurzfassung

Der Bereich der Bioelektronik betrifft die Schnittstelle der Elektronik mit lebenden Systemen. Aufgrund der chemischen Kompatibilität und Funktionalität von organischen Materialien ist die organische Elektronik eine natürliche Wahl als aktives Material für dieses Feld. Das neu entwickelnde Gebiet hat begonnen eine Reihe von in vitro und in-vivo-Sensoren und Detektoren zu erforschen und zu erkennen.

Ausgehend von dieser Motivation, bioelektronische Geräte beziehungsweise Biosensoren zu entwickeln, beschäftigt sich die vorliegende Masterarbeit mit der biologischen Funktionalisierung von organischen Feldeffekt-Transistoren (OFET) und dem Beweis der biologischen Modifikation an der Halbleiteroberfläche. Das Ziel dieser Arbeit besteht darin, Feldeffekt-Transistoren, welche aus organischem, biokompatiblen, günstigem, stabilem und nicht-toxischem Halbleiter bestehen, herzustellen und jene in wässrigem Umfeld mit Biomolekülen auf der Stelle ohne großen Aufwand zu dekorieren und zu operieren, sodass sie als spezifische und selektive Biosensoren verwendet werden können.

Kürzlich sind in unserer Gruppe Halbleiter mit Wasserstoffbrückenbindungen als potentielle Materialien für Bioelektronik entdeckt und entwickelt, die aufgrund ihrer günstigen elektronischen Leistungsfähigkeit, Betriebsstabilität, und das Vorhandensein von chemischen Angriffstellen in Form von Amin und Carbonyl-funktionellen Gruppen vielversprechend sind. Das Pigmentmaterial Epindolidione (EPI) wurde in dieser Arbeit untersucht, und es zeigte sich als aussichtsreiches Material für bioelektronische Zwecke.

Epindolidione wurde in halbleitenden polykristallinen Dünnschichten durch Vakuumaufdampfen verarbeitet. Die Protokolle für die Biofunktionalisierung der Oberflächen wurden im Detail für zwei biologische Systeme untersucht: Die *Rhodobacter sphaeroides* photosynthetischen Reaktionszentrums (RC) und Streptavidin. Für das RC wurde ein Verfahren zur kovalenten Biofunktionalisierung durch die Verwendung eines Korksäure basierten Linkers (SUB) entwickelt. Für Streptavidin wurde ein funktionalisiertes Biotin (B7) Ester als Linker verwendet. Die Biokonjugationsreaktion auf den oberflächenmodifizierten Proben wurde unter Verwendung von Atomkraftmikroskopie (AFM), Wasserkontaktwinkel -Messungen und Fourier-Transformations-Infrarotspektroskopie (FTIR) verifiziert. Mit dieser Kombination

von Methoden wurde das Protokoll für die Oberflächenfunktionalisierung optimiert und die erfolgreiche kovalente Modifikation der Oberfläche bestätigt.

Mit dem Wissen, dass die EPI Filme erfolgreich modifiziert werden können, haben wir uns bemüht, um sicherzustellen, dass sowohl die Protein als auch der Halbleiterfilm ihre jeweiligen Eigenschaften beibehalten.

Zu diesem Zweck haben wir organische Feldeffekt-Transistoren aus EPI hergestellt. Wir haben festgestellt, dass diese Transistorvorrichtungen in wässriger Umgebung bei aggressiven pH Bedingungen (3-10) in Betrieb bleiben. Wir haben uns die Frage gestellt, ob es möglich wäre, OFETs aus Epindolidione zu fabrizieren, jene an der Oberfläche durch biologische Verknüpfungen im wässrigen Umfeld zu funktionalisieren um schließlich damit diverse Proteine detektieren zu können. Würden empfindliche Bauelemente wie OFETs trotz dieser wässrigen Funktionalisierung noch einsatzfähig sein?

Um Antworten auf diese Fragen zu finden, wurden "bottom-gate/top-contact" Feldeffekt-Transistoren aus Epindolidione produziert. Diese wurden im linearen Regime bei niedrigen Spannungen operiert, um unerwünschte elektrochemische Reaktionen in der wässrigen Elektrolytlösung zu vermeiden. Es stellte sich heraus, dass ersichliche Beweise für die Biokonjugation an der Oberfläche vorhanden sind. Die OFETs zeigten unterschiedliches Verhalten vor und nach der Funktionalisierung der Epindolidione-Oberfläche.

Zusammenfassend konnte in dieser Arbeit gezeigt werden, dass die Oberflächenmodifikation des organischen Halbleiters Epindolidione durch kovalente Bindung mit diversen Biomolekülen erreicht wurde. Daher glauben wir, dass nach einer weiteren Gestaltung und Entwicklung Epindolidione in verschiedenen Biosensor-Anwendungen Zugang finden kann. In der nahen Zukunft ist die Funktionalisierung von Epindolidione-Oberfläche mit Neuronen für medizinische Zwecke vorstellbar.

# Acknowledgement

First of all I would like to thank o.Univ. Prof. Mag. Dr. DDr. h.c. Niyazi Serdar Sariciftci , who enabled this master thesis, for his support and advice during the time of my studies.

I am also very grateful to my supervisor Eric Głowacki, MSc. Dr. for his guidance, encouragement and support throughout this work, for his expertise and enthusiasm in the field that motivated me and finally for his patience to teach and coach me through the hard labwork.

Much beneficial work that enhances my thesis was done in collaboration with partners in other institutes and universities. Therefore, I would like to specially thank Alessandra Operamolla and Robert R. Tangorra from the University of Bari, Italy and Rudolf Haßlacher from Johannes Kepler University Linz, Austria for their experimental support.

Also special thanks go to my friends Liviu Dumitru Dr. , Meltem Akcay MSc, and Yasin Kanbur Dr. for their support and especially for small coffee breaks to increase my motivation.

Furthermore I would like to thank all the people at the institute for their fruitful discussions during the group meetings at LIOS, especially Markus Scharber DI Dr. and Philipp Stadler DI Dr.

Finally I want to thank my family, mainly my parents Filiz and Tuncay and my sisters Betül and Tuba Coskun for their faith in me during the whole period of my studies and of course to Eng. Abdalaziz SA Aljabour for his love and encouragement.

# Contents

<b>1</b>	<b>Introduction</b>	<b>9</b>
1.1	Motivation	9
1.2	The development and application of Biosensors	10
1.3	Biological Interactions	12
1.3.1	Substrate and <i>Rhodobacter sphaeroides</i> reaction center (RC)	12
1.3.2	Biotin and Streptavidin	14
1.4	Hydrogen-bonded organic semiconductor: Epindolidione	15
<b>2</b>	<b>Experimental techniques</b>	<b>18</b>
2.1	Surface morphology studies	18
2.1.1	Atomic Force Microscopy (AFM)	18
2.1.2	Contact Angle Measurement	19
2.2	Organic field effect transistors	21
2.2.1	Transistor design and characteristics	21
2.2.2	Operating principle and parameter extraction	23
2.2.3	Device fabrication	25
2.2.4	Surface functionalization with biomolecules	26
2.2.4.1	Substrate and RC functionalization	26
2.2.4.2	Biotin and Streptavidin modification	27

<b>3</b>	<b>Results</b>	<b>27</b>
3.1	Surface functionalization and its verification	27
3.1.1	FTIR Spectra of Epindolidione linked with Suberate and RC	29
3.1.2	FTIR Spectrum of Epindolidione linked with Biotin and Streptavidin	31
3.2	AFM and Contact Angle Measurements	33
3.2.1	AFM and Contact Angle Measurements of EPI films with Suberate and RC modification	33
3.2.2	AFM and Contact Angle Measurements of EPI films with Biotin and Streptavidin modification	35
3.3	OFET characterization	37
3.3.1	Stability of Epindolidione OFETs	37
3.3.2	OFET response to Suberate and RC interaction on the EPI surface	40
3.3.3	OFET response to Biotin and Streptavidin interaction on the EPI surface	41
<b>4</b>	<b>Conclusion</b>	<b>44</b>
<b>5</b>	<b>Literature</b>	<b>47</b>
<b>6</b>	<b>Curriculum vitae</b>	<b>50</b>

# 1 Introduction

## 1.1 Motivation

Bioelectronics gained special significance in recent years. Especially the interdisciplinary information exchange, which means connecting the areas of biology, chemistry, physics and materials science, has made an important contribution for it. Already in the 1980s, bioelectronic devices such as biosensors should satisfy the analytical needs of the world. Such requirements are not only limited to medical science purposes *i.e.* for diagnosing diseases, but extend from the food industry over to the military. Although we face in everyday life different kinds of biosensors and bio-electronic devices, such as pacemakers, pregnancy tests or blood glucose sensors, the science seeks for further development to increase the application field of bioelectronic devices more and more. Basically the features of specificity, selectivity, cost effectiveness and easy usage are required.

In this thesis, an attempt is made to develop a milestone for the next generation of biosensors. A hydrogen-bonded organic pigment of natural origin was examined for surface modification. By existing secondary amine and carboxylic acid groups of the semiconducting pigment, which also occur in our DNA, a bioconjugation between various biomolecules has been achieved. In the present study, 2 prototypes were tested: (a) Suberate and the *Rhodobacter sphaeroides* photosynthetic reaction center (RC); and (b) Biotin and Streptavidin interactions, which can however be replaced depending on the desired biomolecule. The developed model of the surface functionalization seems to be promising.

## 1.2 The development and application of Biosensors

A biosensor is an analytical device which converts a biological response into an electrical signal. The aim of these bioelectronic devices is to couple organic electronics, which concerns with the application of carbon-based semiconductors in the form of conjugated small molecules, with the biological world. Two parts can be distinguished during this coupling process: (a) where a biological reaction transfers a signal to an organic electronic device; (b) or an organic electronic device triggers a biochemical reaction [1,2].

The utilization of electronic devices in biology and medicine is not new. Already in 1791 an Italian physician and natural scientist announced that electricity was inherent in organic tissue. Luigi Galvani made a fundamental contribution to modern electrocardiography due to his experimental findings of electrical phenomena in frog muscles and hearts [3]. From that time the research activity in this confluent field has grown rapidly. With the development of microelectronics in the 1950s-1960s implantable devices for the stimulation of the organs were introduced (*e.g.* pacemaker) [4]. In the past few years, organic field-effect transistors (OFETs) have played an important role in biosensing. Many different research groups have been investigating OFETs in various applications. Some examples can be listed as the DNA-sensing, chirality distinction of compounds and the detection of molecules, known to human body[5,6,7].

As clearly seen from the research interest, the integration of modern electronics with biology and medicine has made and will also make in the future a technological advance. The design and development of bioelectronic devices is shown in Fig.1. The improvement of semiconductor technologies and the miniaturization of semiconductor devices is of great importance for biomedical applications. It is anticipated that small, economical, reproducible biosensors made out of organic semiconductors will dramatically lower the medical costs [4].

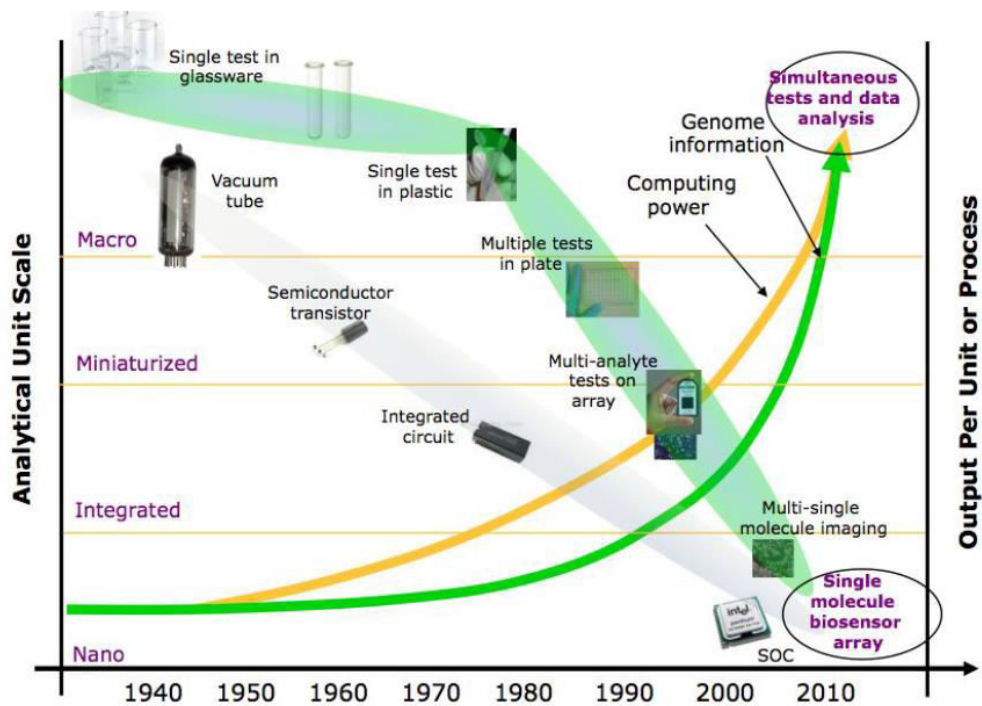


**Figure 1:** The design and development of bioelectronics [4]

In the future, nanoscale bioelectronics and highly integrated systems are in highlight for the next generation of research. Thus, this may allow a personalized-medicine in the sense of medical diagnoses without the requirements of infrastructure and trained operators [4].

## 1.3 Biological interactions

### 1.3.1 Suberate and *Rhodobacter sphaeroides* reaction center (RC)

In this chapter the interaction of the aliphatic linker disuccinimidyl suberate with the *Rhodobacter sphaeroides* R26 reaction center (RC) is introduced [8].

The chemical structure of disuccinimidyl suberate is shown in Fig. 2 below.

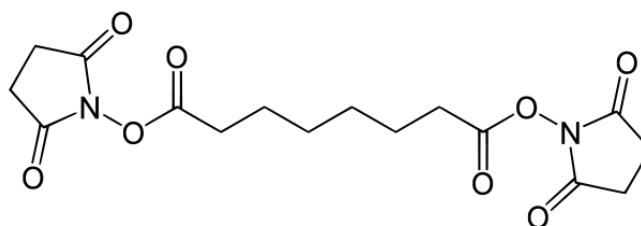


**Fig.2:** The chemical structure of disuccinimidyl suberate

In biological chemistry this compound is a common tool used as protein-crosslinking agent. The function of the *N*-succinimidylester (NHS) on the linker is to couple to molecules which contain amine groups [8]. NHS is a good leaving group, which makes the NHS ester an electrophile suitable for attack by nucleophiles such as amine groups.

Especially the interaction of the succinimidylester functionality with the *Rhodobacter sphaeroides* reaction center (RC) has been evaluated before[9].

As discussed in previous chapters, making use of biological knowledge in chemistry and physics was always an attractive issue. In the last few years another research direction gained interest: making use of bacteria for physical phenomena. The construction of artificial photosynthetic media for the conversion of solar energy into electrical energy was achieved by using photosynthetic organisms [9].

*Rhodobacter sphaeroides* reaction center (RC) is a bacterial photoconverter. It is a membrane-spanning protein with the ability to convert photon absorption into charges in the photosynthetic process. An illustration of RC is shown in Fig. 3 [9].

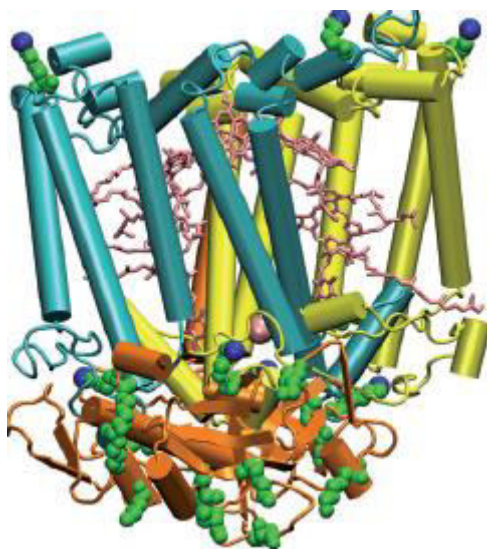


**Fig.3:** Rhodobacter sphaeroides reaction center (RC) [9]

The protein matrix consists of 9 cofactors: 2 ubiquinonenes ( $UQ_{10}$ ;  $Q_A$  and  $Q_B$ ), 1 iron ion, 2 bacteriopheophytins and 4 bacteriochlorophylls, two of which mould a functional dimer (D). Upon photon absorption, one electron of D is excited and transferred to the electron acceptor quinone  $Q_A$  and finally  $Q_B$ . A charge recombination reaction can occur in a timescale from milliseconds up to seconds if external reductants are absent. Furthermore 22 lysines (Lys) are found in RC, 9 of which are responsible for the bioconjugation targets due to their positions. The light harvesting properties of this protein were investigated in detail in the cited literature [9].

In this thesis, the bioconjugation protocol was applied in another context. The interaction of RC with the disuccinimidyl suberate linker was used in order to modify the organic semiconductor surface.

### 1.3.2 Biotin and Streptavidin

Biotin, also known as vitamin H, belongs to the group of vitamin B. It plays an important role in the body in metabolic processes, carboxylations, and the citric acid cycle. Once suffering from biotin deficiency, symptoms like anorexia, fatigue and depression can occur. Therefore, it is important to take biotin in the diet. The daily requirement for adults is between 30-60 micrograms and can be supplied by egg yolk, soybeans and dry yeast. The chemical structure is presented in Fig.4 [10].

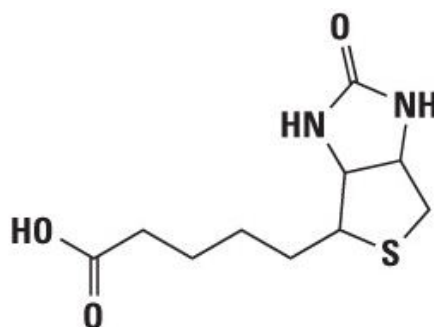


Fig. 4: Chemical structure of Biotin [10]

The binding of biotin to the streptavidin was first discovered in 1941 by Esmond Snell and co-workers and is considered as one of the strongest non-covalent binding with a dissociation constant of  $10^{-15}$  M [11].

Streptavidin, synthesized by bacteria called *Streptomyces avidinii*, is a protein that is similar to avidin. Streptavidin is not a glycoprotein as compared to avidin and can therefore respond to non-specific binding. Due to the absence of carbohydrates and an isoelectric point at 5, streptavidin has a lower solubility in comparison to avidin. Moreover, it is composed of 4 identical subunits. Each subunit consists of 159 amino acids and is capable of binding a biotin molecule. The binding mechanism of biotin to streptavidin is shown in Fig. 5 [10,11,12].

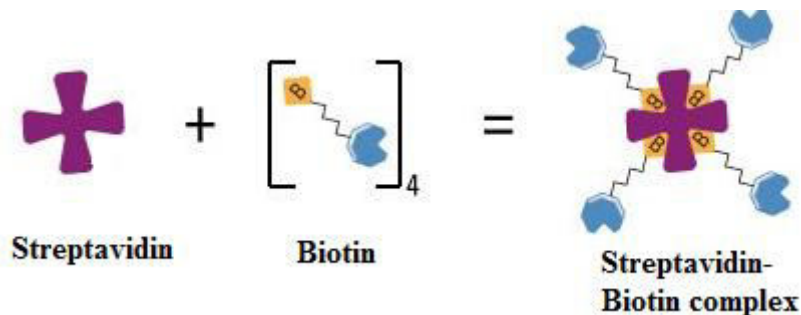


Fig.5: Binding mechanism of biotin to streptavidin [10]

Nowadays, biomedical applications make use of the strong affinity of streptavidin to biotin for instance in fluorescence microscopy in detection of proteins, Western blotting and ELISA (enzyme linked immunosorbent assay) test [10].

## 1.4 Epindolidione

In recent years some hydrogen-bonded organic pigments have emerged as promising semiconductor materials. Their low-cost and non-toxicity makes them good candidates for biocompatible electronics. They have been found to operate stably in aqueous environments. One promising pigment material is Epindolidione [13].

Epindolidione, derived from Indigo via thermal rearrangement at high temperatures, is a four six-membered ring system as presented in Fig. 6 [14].

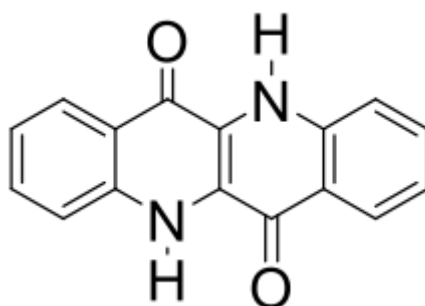
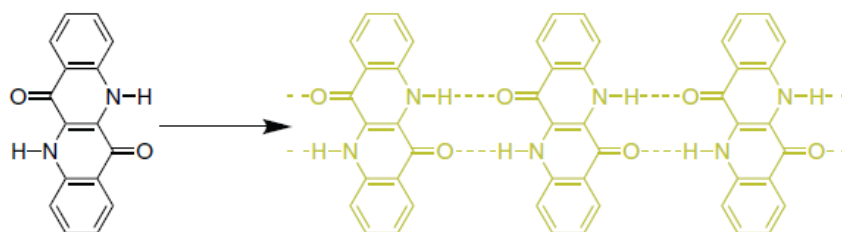


Fig.6: Hydrogen-bonded organic semiconductor Epindolidione

It was first synthesized in 1934 in order to imitate indigo. Despite original expectations, this yellow and highly fluorescent pigment was not consistent in its properties with indigo. Only after 1960 epindolidione gained interest in parallel with structurally-related, commercial pigment quinacridone [14].

The resonance structure of epindolidione featuring enol or imine character is thermodynamically unfavoured, at neutral pH conditions. Since carbonyl and amine groups break the conjugation in the system, they can be classified as less conjugated than their analogous acenes. However, there are intermolecular hydrogen bonds between the amine (-NH-) and carbonyl groups (C=O) of the neighbouring molecule in epindolidione (Fig.7), leading to remarkably stable organic semiconductor properties with a charge carrier mobility of  $1.5 \text{ cm}^2/\text{Vs}$  [13].



**Fig.7:** Intermolecular hydrogen-bonds between the carbonyl and amine groups [13]

The presence of amine, carbonyl and hydrogen-bonding groups are quite similar to the functional groups found in biology, in particular in peptides/proteins. Deoxyribonucleic acid (DNA) is probably the best example of the interplay of these 3 groups [15].

Based on this motivation, to find the network of all 3 linking sites ((-NH-), (C=O) and (-NH-O=C)) in the organic semiconductor pigment, it has been attempted to carry out a surface modification on the epindolidione with a commercially-available bioconjugation linker in order to investigate protein interaction on the semiconductor surface.

The binding mechanism of both aliphatic linkers (suberate and biotin) with the *N*-succinimidyl functionality and the hooking principle of the corresponding protein is illustrated in Fig. 8.

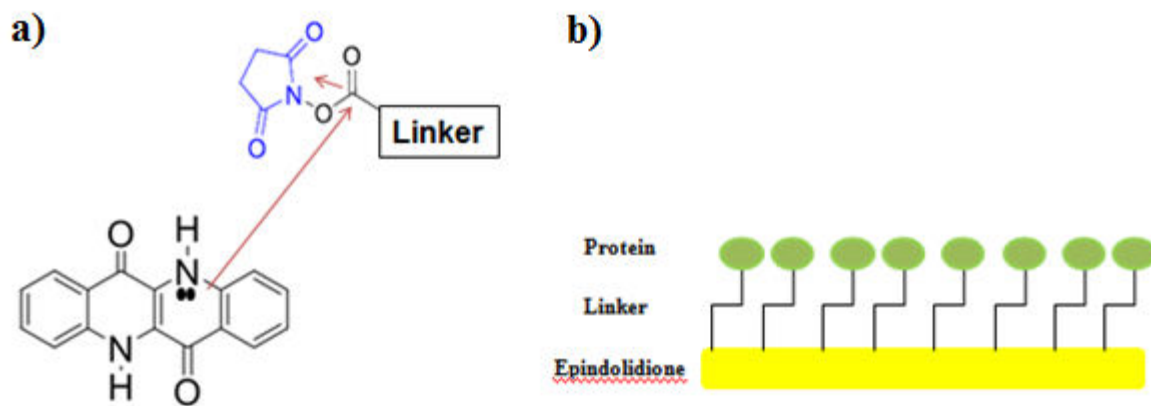


**Fig.8:** a) Proposed binding principle of the organic semiconductor Epindolidione to the linker via nucleophilic attack. For both, suberate and biotin, the binding mechanism is the same b) The linker in between epindolidione and protein, connecting the electronic world with the biological one

The surface decoration procedure consists of 2 steps: in the first step the lone-pair of amine of epindolidione makes a nucleophilic attack on the carbonyl group of the linker, resulting in a new amide linkage and having NHS as a leaving group. Next, the proteins with a high affinity are hooked on the linkers other side via nucleophilic attack by lysine, building a bridge between the organic semiconductor and the protein [8].

From previously published results, it was found that epindolidione is a suitable candidate for biosensing applications, due to its operational stability in both air and aqueous environment. The material was tested in an OFET structure at harsh pH conditions from pH 3-pH 10 and remained working after hundreds of cycles of measurement. Thus, all these properties together making hydrogen-bonded semiconducting pigment epindolidione applicable in biocompatible electronic devices [16,17].

## **2 Experimental techniques**

### **2.1 Surface morphology studies**

#### **2.1.1 Atomic force microscopy (AFM)**

The atomic force microscopy (AFM) is a high resolution microscopical technique with nanometer-scale resolution. It belongs to the category of Scanning Probe Microscopy (SPM) techniques [18].

The first invention of the SPM techniques started with the Scanning Tunneling Microscope (STM) by G. Binnig and H. Rohrer, for which they were recognized with the Nobel prize for Physics in 1986. By further development in the same year AFM was invented by G.Binnig, C.F.Quate and Ch. Gerber [19].

In AFM several properties can be investigated such as topographic images, roughness determinations, mechanical, magnetical, electrical, optical and thermal surface and interface properties, depending on which kind of force is applied.

An AFM consists of a cantilever, typically made out of silicon or silicon nitride, with a tip at the end of it. A constant force is applied between the sample and the tip, which allows one to monitor the motion of the sample as it is scanned over the surface, leading to a 3-dimensional image of the surface [20].

Basically, two operation modes can be distinguished in AFM: namely contact mode and non-contact mode. In the contact mode AFM, a very soft cantilever tip is brought in contact with the sample. In this operation mode the repulsion forces between the probe and tip are measured, whereas in the non-contact mode the cantilever does not touch the sample. Here, a stiff cantilever oscillates above the surface of the probe at such a distance that the repulsive regime is not valid anymore and only attractive Van-der-Waals interactions occur. In this mode the force is obtained by comparing the frequency and or the amplitude of the cantilever oscillation relative to the driving signal. A comparison of these two operation regimes is shown in Fig. 9 [18,20,21].

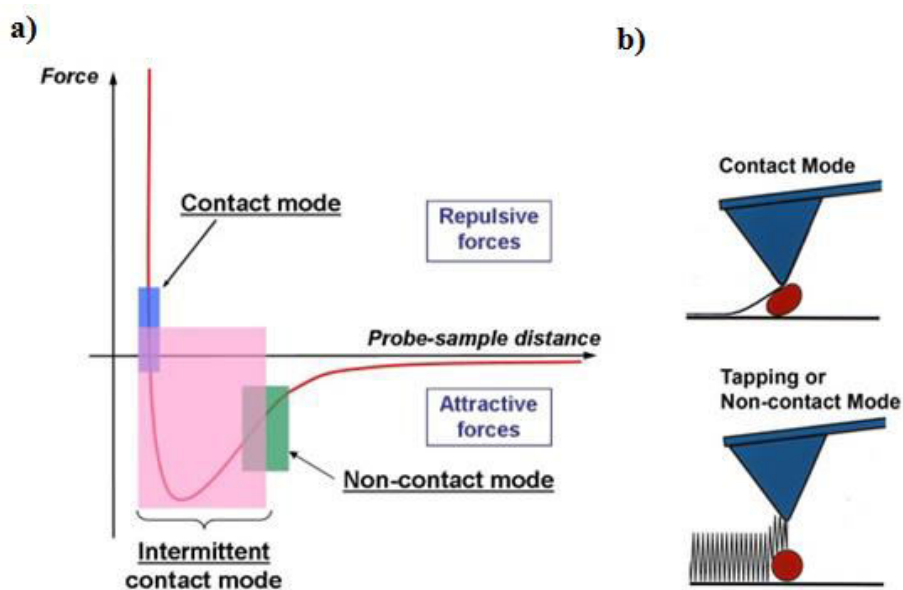


**Fig.9:** a) Comparison of the 2 operation modes in the AFM and b) illustration of them [20,21]

For this current study, the AFM technique was used in order to follow the surface modifications on the semiconductor before and after every treatment step of the evaporated epindolidione films on silanized glass. A Park XE-100 SPM microscope was used in a non-contact tapping mode with a cantilever of 125  $\mu\text{m}$  length and a tip of PPP-NCHR. A 330 kHz resonance frequency, 42  $\text{N m}^{-1}$  nominal force constant, less than 10 nm tip curvature radius and a scan rate of 1 Hz were used throughout the measurements. The obtained topography data were analyzed with the software XEI, Park system cooperation 1.8.0 [8].

### 2.1.2 Contact Angle Measurement

Among many other methods contact angle determination is an important technique for the investigation of the wettability of surfaces. It is described as the angle, formed at the liquid-solid and liquid-vapor interface [22].

If the contact angle is small ( $<90^\circ$ ), the liquid droplet spreads on the surface and a high wettability is achieved, whereas a large contact angle ( $>90^\circ$ ) corresponds to low wettability as shown in Fig.10 [23].

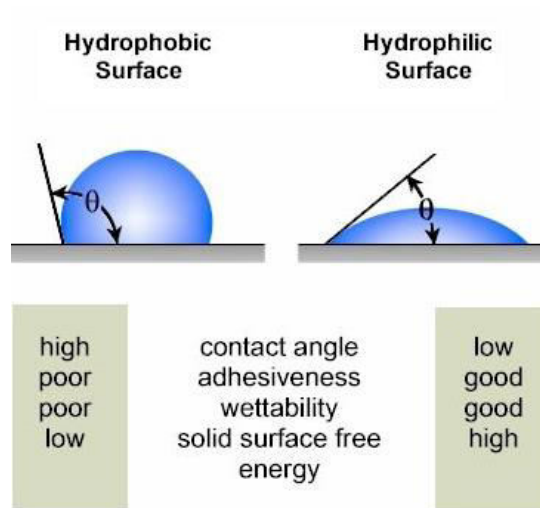


**Fig.10:** The effect of a liquid droplet on the surface properties [22]

Generally, the form of a liquid droplet is influenced by the surface tension of the liquid. Described by Young's equation, a correlation between the contact angle of a liquid drop and the solid surface under the interaction of three interfacial tensions are found. In Fig.11 the Young's equation is presented [22].

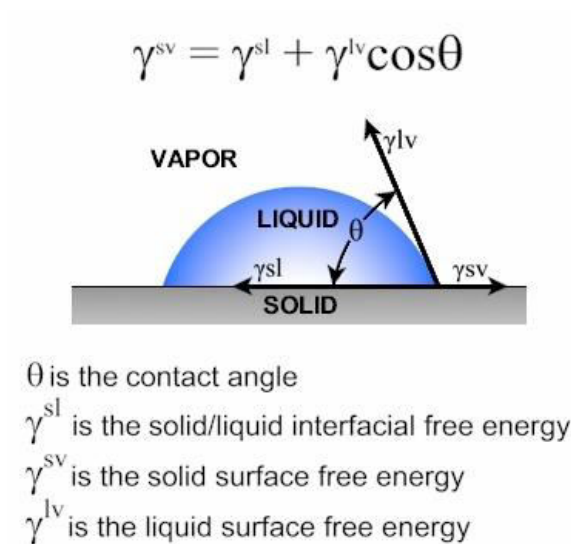


**Fig. 11:** Young's equation describing the relationship between the liquid, solid and interfacial tensions [22]

Basically, the contact angle  $\theta$  can be determined by many different ways but three of them are well established, which are a) dynamic contact angle measurement, via adjusting the volume of the droplet or tilting cradle; b) the force tensiometry and c) the optical tensiometry.

In the force tensiometry the mass is measured which affects the balance at the interface where the sample meets the test liquid. By knowing the surface tension of the liquid and the perimeter of the sample the contact angle can be obtained.

In optical tensiometry a liquid droplet is brought onto the solid surface and the image of the droplet is taken. Besides other fitting methods such as circle and polynomial, the Young-Laplace equation is the most common used fitting for the determination of the static contact angle [23].

## **2.2 Organic field-effect transistors (OFETs)**

### **2.2.1 Transistor design and characteristics**

The invention of the transistor by John Bardeen, William Shockley and Walter Brattain in 1947 was a milestone in the development of modern electronics. Due to some technological limitations of inorganic electronics, organic-based devices have newly emerged in the market, and have great possibility to find their place in a wide range of new applications.

Organic field-effect transistors (OFETs) are based on thin films of organic semiconductors, and are seen as highly-advantageous for many low-cost, large area and flexible devices, including electronic papers, radio frequency identification (RFID) tags, and chemical and bio sensors [24,25]. Especially the utilization of OFETs in biosensor technologies is a major topic of research and development in recent years. The motivation for applying organic field-effect devices to biological sensing is various: simple processing, operation in wet environment, compatibility of flexible and large area substrates and the production of OFETs of highly chemically-tunable active layer materials make them ideal candidates for bio-detection [5,6].

Organic field-effect transistors can be fabricated in many different configurations, as shown in Fig. 12 [26].

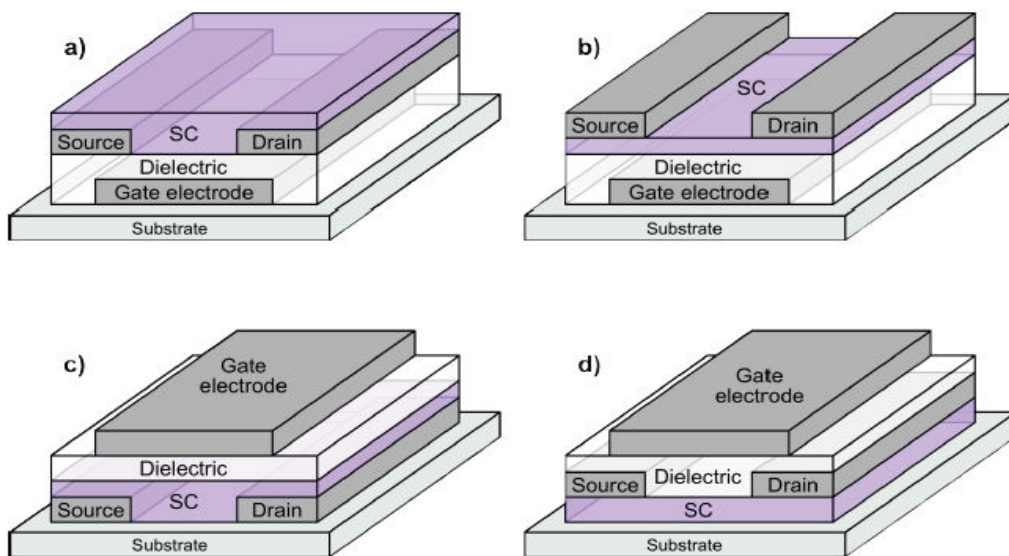


**Fig:12:** The structure of different OFET configurations: a) bottom-gate bottom-contact, b) bottom-gate top-contact, c) top-gate bottom-contact, d) top-gate top-contact [26]

The most common and well-established geometry is the bottom gate-top contact configuration. In this work, the gate consisted of a vacuum-evaporated aluminum layer with an electrochemically-grown aluminum oxide dielectric layer on top [14]. The gate dielectric was modified with a thin (10-20 nm) layer of an organic aliphatic material such as oligoethylenetetracontane (TTC) or polyethylene (PE). This layer functions to achieve a low surface energy to facilitate the proper growth of the subsequently-deposited organic small molecule semiconductor and also to passivate harmful surface states present on the oxide. The electronic functionality of the transistor is largely determined by this gate dielectric structure. The number of charge carriers in the channel and therefore the operating voltage of the device depends on the capacitance of the dielectric. Furthermore the surface properties of this layer determines the molecular growth and the orientation of the organic semiconductor which is deposited on top of it.

The semiconducting material can be deposited by different methods onto the device, for instance via spin-coating for soluble polymers or vacuum evaporation for small molecules. The organic semiconductor epindolidione, which was used throughout this study, was deposited by evaporation. A physical vapor deposition evaporator was used, in which the material is resistively heated in a crucible. The evaporation starts when the chamber is evacuated. The sublimed material condenses on the substrate. The film thickness can be

controlled through monitoring the substrate temperature and the deposition rate using a quartz crystal microbalance [26]. The source-drain electrodes were finally deposited by physical vapor deposition. These electrodes consisted of gold, evaporated as a rate of  $0.3 \text{ \AA s}^{-1}$  to a thickness of 60 to 80 nm.

## 2.2.2 Operating principle and parameter extraction

The creation of the free charge carriers at the gate dielectric-semiconductor interface is achieved after a voltage is applied to the gate electrode in order to polarize the dielectric layer. According to the applied gate voltage a shift of the energy levels in the semiconducting material occurs as shown in Fig. 13. Also depending on the work function of the source-drain metal electrodes and the polarization properties of the capacitor- acting dielectric, a certain amount of charges is injected from the source to the semiconductor and a conductive channel arises [26,27].

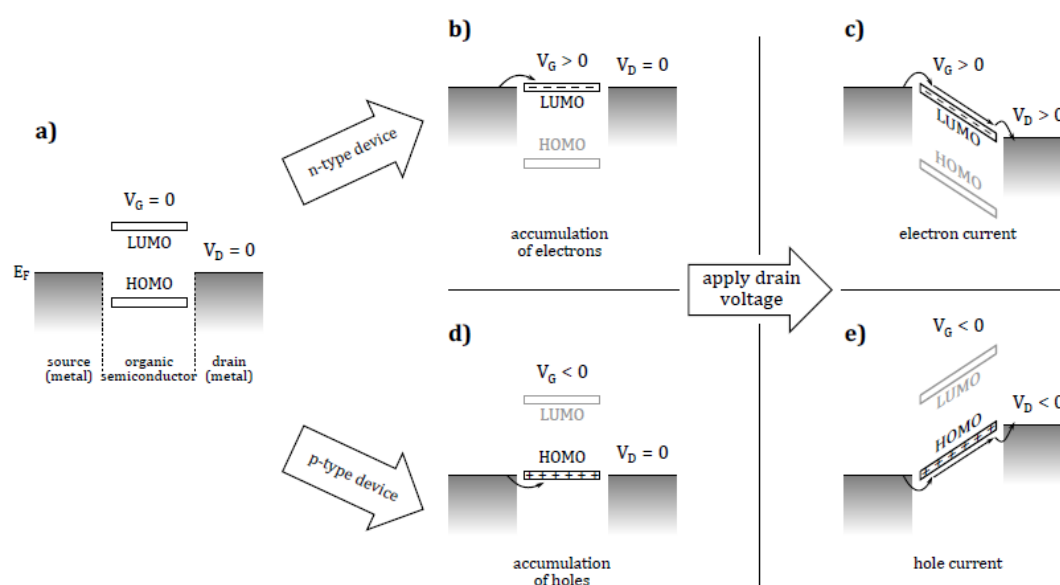


**Fig.13:** OFET working principle with respect to applied gate voltage: (a) No charges injected when  $V_g = 0$  V, (b) injection of electrons to LUMO (n-type) of the organic semiconductor (c) current flow of electrons with an applied positive drain voltage (d) injection of holes to HOMO (p-type) and (e) current flow of holes with an applied negative drain voltage [26]

Depending on the applied voltage, two different methods are used for the characterization of OFETs: Either the gate voltage is kept constant and the source-drain voltage is changed (output characteristics) or vice versa where the source-drain voltage is held constant and the gate voltage is swept (transfer characteristics) [26,27].

The electron-enhanced mode is developed by applying positive source-drain and gate voltages, whereas hole-enhanced mode is achieved with negative voltages. The intercept of the extrapolated linear curve with the gate voltage-axis in the transfer characteristics shows the threshold voltage, the minimum gate voltage that is essential to form the conducting channel [28].

Further, three operation regimes can be distinguished in an field-effect transistor, namely linear, pinch-off and saturation regimes as shown in Fig.14 [28].

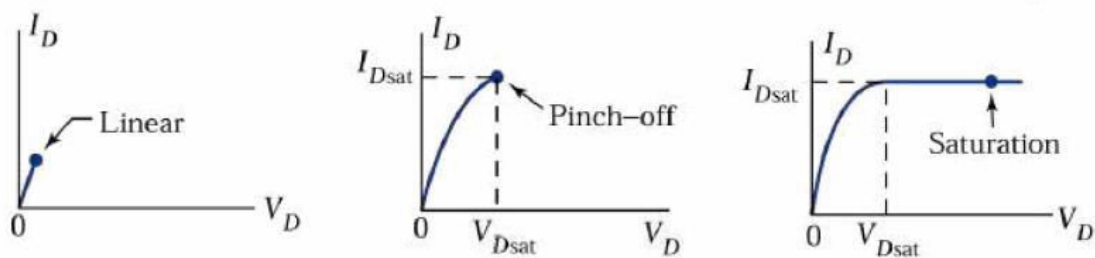


**Fig. 14:** Operation regimes of a field-effect transistor. Figure taken from: [28]

In the linear regime the gate potential is set to a value higher than the threshold voltage. Due to the accumulation of the carriers, a conductive channel is formed. Upon applying a drain voltage the drain current follows linearly the increase of the drain voltage. If the drain voltage is increased further the linear correlation ends and the depletion layer increases and the pinch-off point occurs, at which the drain voltage is higher than gate and threshold voltages ( $V_d = V_g - V_{th}$ ). A saturation current can flow across the depletion zone as carriers are swept from the pinch-off point to the drain by the comparatively high electric field in the depletion region [28].

OFET devices can be used to calculate the mobility of charge carriers in the organic semiconductor. This fundamental materials property can be extracted when the device

geometry, width, length and the capacitance respectively are known, as well as the applied voltages. Three methods exist for the determination of the mobility. Although there is some disunity in the transistor society about which methods are most appropriate, the most common technique for the mobility extraction consists of plotting the square root of the drain current in the saturation regime versus the gate voltage, shown in equation (1) [26, 28].

$$\sqrt{ID_{sat}} = \sqrt{\frac{W \cdot C_i}{2 \cdot L}} * \sqrt{\mu} * (V_g - V_{th}) \quad (1)$$

### 2.2.3 Device fabrication

Organic field-effect transistors used throughout this work for applying the hydrogen-bonded pigment epindolidione for bio-detection applications were fabricated in bottom-gate/top contact configuration. A 100 nm thick aluminum film was used as the gate electrode, evaporated onto glass through a steel shadow mask at a rate of  $10 \text{ A s}^{-1}$ . Next a thin aluminum oxide layer, serving as the gate dielectric, was grown electrochemically on aluminum. The dielectric layer was grown according to the well-established potentiostatic method. The potentiostatic oxidation was conducted in a cell, which was made up of a stainless steel cathode, the aluminum film as anode, and a 0.1 M buffered citric acid / sodium citrate acting as the electrolyte solution. Both electrodes were connected to a Keithley source measurement unit. The anodization ratio for aluminum oxide is known to be  $\sim 1.6 \text{ nm/V}$  [29]. By applying +5V, the potentiostatic anodization would lead to approximately 8 nm of aluminum oxide layer. After the electrochemical oxide growth, the samples were washed with  $18 \text{ M}\Omega$  water, dried and annealed at  $120^\circ\text{C}$  for 20 minutes [14]. Afterwards, a 5 nm passivation layer of the oligoethylenetetracontane ( $\text{C}_{44} \text{H}_{90}$ , TTC) was evaporated onto the  $\text{AlO}_x$  dielectric layer and annealed at  $70^\circ\text{C}$  for 30 minutes in order to obtain a low surface energy and enhance the growth of large crystallites of the organic semiconductors. Thus is necessary to get a good charge transport through the device. Next, 40 nm of epindolidione was evaporated at the rate of  $0.3 \text{ A s}^{-1}$ . Finally, the source and drain electrodes of gold were evaporated through a shadow mask with a width of  $W = 2 \text{ mm}$  and length of  $L=50 \text{ }\mu\text{m}$ . No further passivation was used on the gold electrodes. In order to prevent any electrochemical reactions of the source and drain electrodes in the aqueous environment the OFETs were operated in the linear regime with low source and drain (0.1-0.5V) and gate voltages (3-3.5V)

[8,16]. The OFET schematic as well as the picture of the device during the measurement in wet environment is shown in Fig. 15.

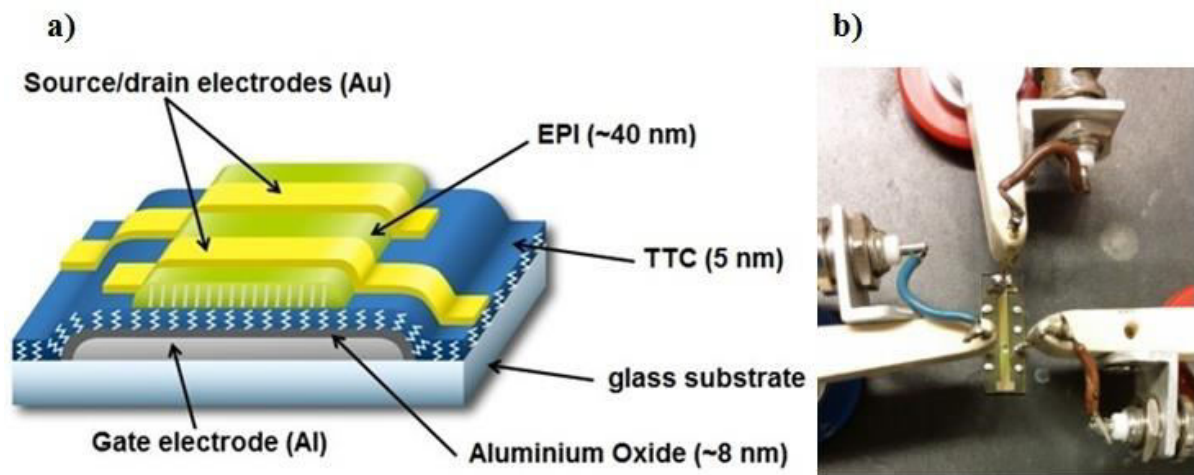


**Fig.15:** (a) Bottom-gate/top-contact configuration of the OFET, (b) a picture of the OFET device connected via gate and source drain electrodes. The measurement was conducted in aqueous environment

## 2.2.4 Surface functionalization with biomolecules

### 2.2.4.1 Substrate and RC functionalization

For the bioconjugation of the *Rhodobacter sphaeroides* reaction center (RC) with the substrate (SUB) linker the following protocol was applied: first a 15 mM stock solution of SUB in dry DMSO was prepared. Next, the stock solution was diluted to 1 mM concentration in 50 mM potassium phosphate, 100 mM KCl at pH 7.2 (PBS). The incubation of SUB as well as RC was conducted in the same way and order for each kind of measurement at room temperature for 4 hours in a sealed, humid petri dish. For AFM and contact angle measurements glass substrates were silanized by treatment with *n*-octyltrichlorosilane (OTS) vapor in a sealed beaker at 90°C for 12h. For FTIR measurements ITO substrates were treated with 5mM octadecyltriethoxysilane in Toluene for 12h and rinsed afterwards with isopropanol and 18MΩ water. OFETs, silanized glass and ITO substrates with epindolidione were first incubated with SUB and washed with deionized water. Afterwards, 30 μL of 20 μM RC in PBS containing LDAO 0.025% v/v were brought onto the surface for further incubation. Finally the samples were rinsed with PBS and deionized water [8].

#### 2.2.4.2 Biotin and Streptavidin modification

Nearly the same bioconjugation protocol was applied for biotin and streptavidin as described in the previous chapter. For this a 3 mM of *N*-succinimidyl biotinate was prepared in DMSO. The stock solution was then diluted with distilled water 20:1 v/v to a concentration of 0.15 mM. Next, this solution was addressed onto the surface of OFETs, silanized glass and ITO substrates with epindolidione in order to functionalize the organic semiconductor. The incubation was carried out for 4 hours at room temperature in a humid environment. Afterwards, the biotin drop was removed, the surface was rinsed with distilled water and was further incubated with streptavidin, diluted to a concentration of 50  $\mu$ M in phosphate-buffered saline PBS. Finally, the samples were washed with PBS and deionized water [8].

### 3 Results

#### 3.1 Surface functionalization and its verification

Untreated epindolidione films were characterized by FTIR spectroscopy on silanized ITO glass substrates, shown in Fig.16. A Perkin Elmer Spectrum One FTIR spectrometer equipped with the specular reflection device *AmplifyIR* was used for the measurements. The spectral resolution was selected as 4  $\text{cm}^{-1}$  and the background spectrum was acquired using a neat ITO slide. The peak assignment is listed in table 1 [8]. The functionalization of epindolidione films with biomolecules as well as the washing steps were followed by FTIR spectra as discussed in the next chapters.

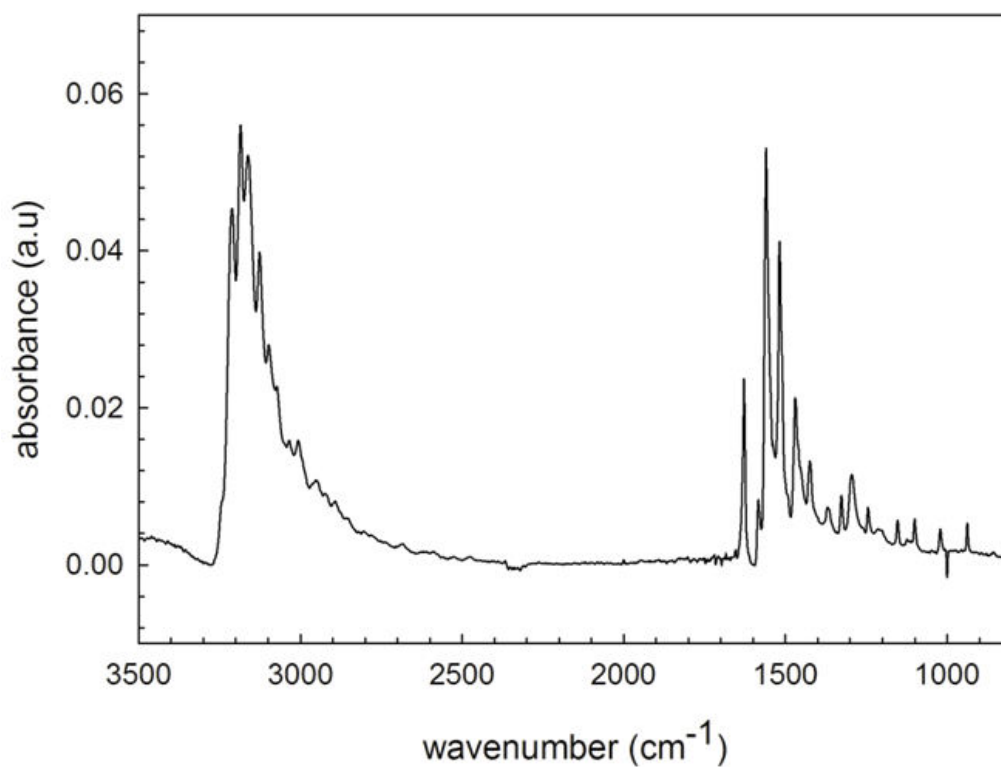


**Fig.16:** FTIR spectrum of pristine epindolidione evaporated on silanized ITO glass substrate

**Table 1:** Peak attribution according to epindolidione by Spectrum v5.0.1 software (Perkin Elmer); ( $\nu$  stretching,  $\delta$  deformation, s symmetric, as asymmetric, s strong, m medium, b broad)

Wavenumber (cm <sup>-1</sup> )	Peak attribution
3215 (s)	$\nu_s$ NH
3164 (s)	$\nu_s$ NH
2930-3110 (b)	$\nu_s$ CH <sub>arom</sub>
1628 (s)	$\nu_{as}$ C=O
1585 (m)	$\nu$ C=C, $\delta$ NH
1560 (s)	$\delta$ NH, $\nu$ C=C
1519 (s)	$\nu$ C=C, $\delta$ CH
1470 (m)	$\nu$ C=C, $\delta$ CH
1428 (m)	$\nu$ C-H
1329 (b)	$\nu$ C-H
1300 (b)	$\delta$ NH, $\delta$ CH <sub>arom</sub>
1246 (b)	$\nu$ C-N, $\delta$ CH <sub>arom</sub>
1156 (b)	$\delta$ CH <sub>arom</sub>
940 (b)	$\delta$ C-C-C <sub>arom</sub> , $\delta$ CH

### 3.1.1 FTIR Spectra of Epindolidione linked with Suberate and RC

The investigation of the functionalized epindolidione surface with SUB and RC was followed by the FTIR spectroscopy. Fig. 17 (a) shows the FTIR spectrum of the organic semiconductor evaporated on ITO-coated glass slides with characteristic peaks corresponding to C-C bonds of the aromatic system as well as the C=O and N-H functional groups, from which the peak assignment is listed in Table 1.

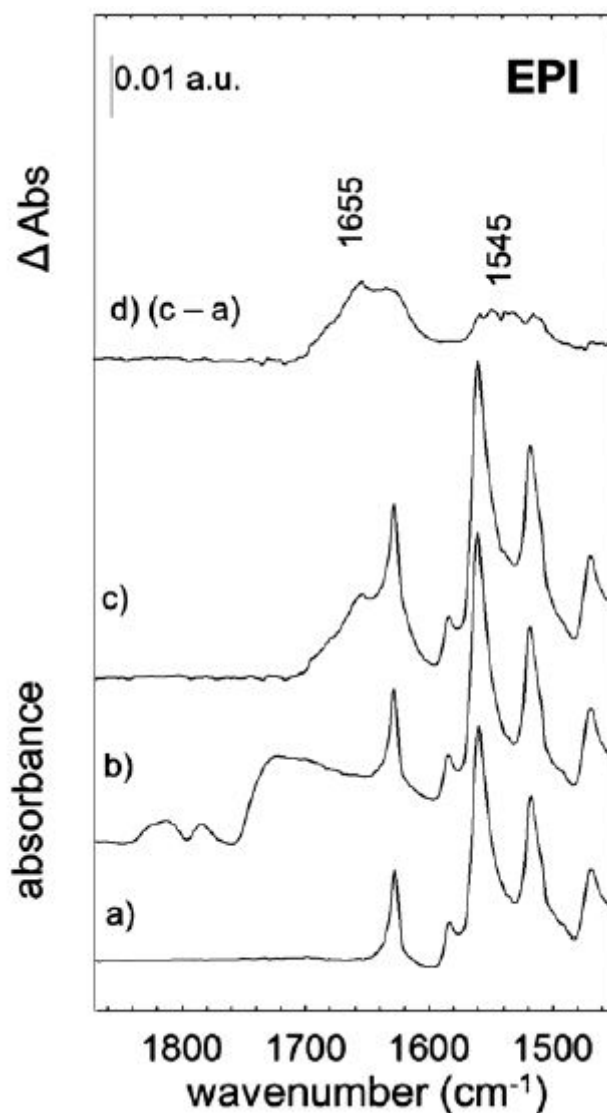


**Fig. 17:** Progression of the bioconjugation of hydrogen-bonded semiconductor epindolidione with SUB linker and the corresponding protein RC, (a) pristine epindolidione, (b) SUB linked to epindolidione, (c) RC hooked to the bioconjugated epindolidione-SUB system, (d) evaluated difference between spectra (c) and (a)

After the incubation of the epindolidione film with the SUB linker (Fig.17b), in which the anticipated nucleophilic attack of the NH group in the semiconductor to the carbonyl group of the linker occurs (Fig. 8a), three new peaks appear. These pronounced signals at 1814, 1784, and especially 1725  $\text{cm}^{-1}$ , corresponding to the stretching vibrations of the two C=O in the succinimidyl ring and to the C=O ester, are a clear evidence of the surface modification of epindolidione with SUB. The further incubation of the epindolidione-SUB bioconjugated system with RC (Fig.17c) results in 2 additional peaks at 1655 and 1545  $\text{cm}^{-1}$ , the so called amide I and amide II peaks of the protein, and the observed signals of SUB disappear. Finally in Fig. 17d the absorption difference of the spectra (a) and (c) are compared, showing strongly the amide coupling of SUB and RC on the semiconductor surface.

For a better understanding, if the RC is really coupled via covalent bond or only physisorption, the FTIR spectrum of the pristine and bioconjugated epindolidione was taken (Fig. 18) after several washing steps with phosphate buffered saline PBS. It is clearly shown that for bioconjugated RC, no absorption differences were observed after 2 rinses in PBS (Fig. 18a), whereas for physisorbed RC, no absorption signals were detected after the first rinsing (Fig. 18b), indicating any unspecific interaction with the hydrogen-bonded organic semiconductor.

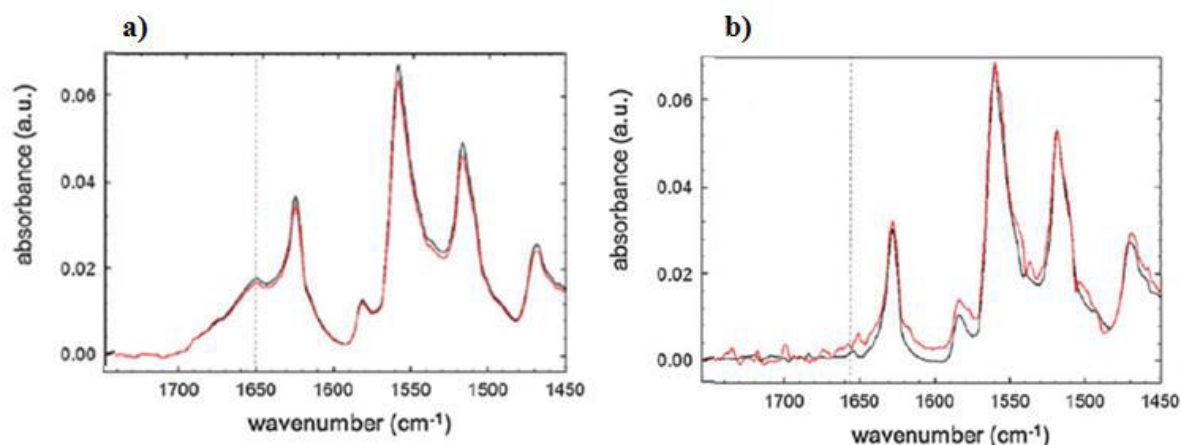


**Fig. 18:** Evaluation of physisorbed and bioconjugated RC on epindolidione-substrate by washing procedure with phosphate buffered saline, (a) bioconjugated RC, (b) physisorbed RC

Thus the FTIR spectra show obviously the bioconjugation of the RC to the hydrogen-bonded semiconductor pigment in comparison with only physisorbed RC.

### 3.1.2 FTIR Spectra of Epindolidione linked with Biotin and Streptavidin

The bioconjugation of the hydrogen-bonded organic semiconductor epindolidione (EPI) with the succinimidyl biotinate (B7) linker was investigated through FTIR spectroscopy as well.

Fig.19 represents the IR spectra of the pristine biotin and epindolidione in comparison to the biotin incubation and PBS washing on the semiconductor pigment surface. The IR spectra in Fig. 19a shows once more only epindolidione, whereas in Fig. 19b pristine biotin is presented with the peaks at 1817, 1790, 1749, and 1730  $\text{cm}^{-1}$  corresponding to the two C=O functionalities on the succinimidyl group and to the ester carbonyl. Furthermore the stretching of the biotin ureido carbonyl was recorded at 1700  $\text{cm}^{-1}$ . Following the biotin incubation, a new signal was observed at 1600  $\text{cm}^{-1}$  (Fig. 19c), corresponding to the amide bond absorption, whereas no peaks were found at 1817 and 1790  $\text{cm}^{-1}$ , suggesting the complete reaction of the NHS ring. Moreover, the broad signal at 1600  $\text{cm}^{-1}$  can be deconvoluted into three peaks: one at 1600  $\text{cm}^{-1}$  associated to the semiconductor, the other one at 1715  $\text{cm}^{-1}$  belonging to the ureido carbonyl stretching, which is not responsible for the covalent binding, and the last one at 1650  $\text{cm}^{-1}$  suitable for the amide binding. With this information it can be reasonably concluded that the covalent binding of the biotin on the nitrogen atom was successfully achieved.

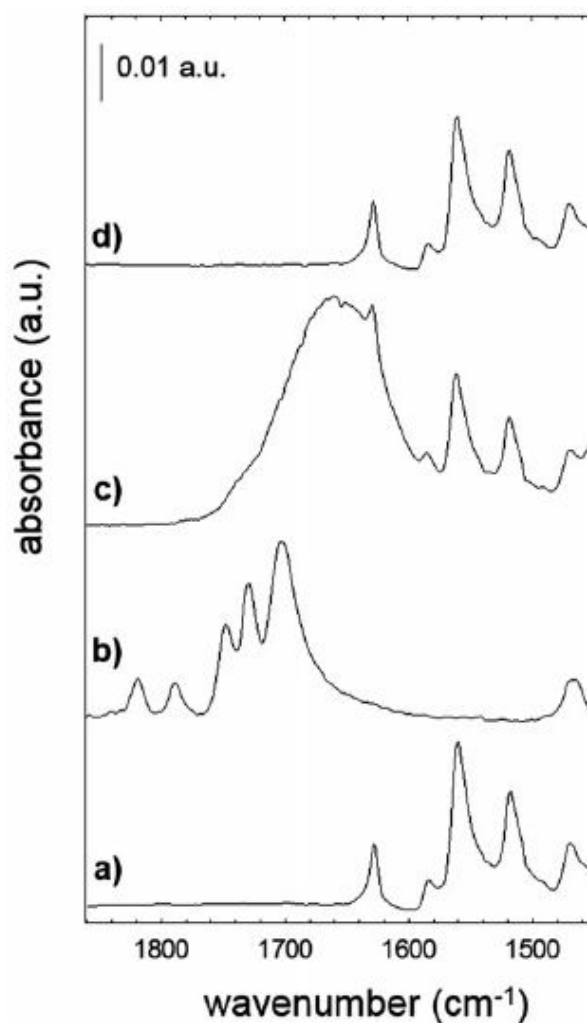


**Fig.19:** The sequence of the bioconjugation on the epindolidione semiconductor surface with biotin linker, (a) pristine epindolidione, (b) pristine biotin, (c) organic semiconductor film incubated with biotin, (d) washing step after the biotin incubation

The same washing procedure with PBS, as done in the substrate case, was conducted for biotin as well, however it turned out that the peaks corresponding to the biotin disappeared in the IR spectra (Fig. 19d). Due to the vanishing of the biotin signals after washing, one could believe that the linker is detached from the semiconductor surface, however from the previously published results in the literature about biotin immobilization it is reported that these signals disappear during aqueous washing procedure although the linker is still present. The reasons for this disappearance were explained as shielding or other changes in the environment affecting the vibrational properties of the ureido ring [30,31]. In our experiments, no difference was recorded between the IR spectra in Fig. 19a and d, because the spectral range of interest was covered by the semiconductor peaks [8].

Nevertheless, the bioconjugation on the epindolidione surface with biotin via covalent binding can be supported not only by FTIR spectroscopy, but also by AFM and especially by OFET studies as described in the following chapters.

## 3.2 AFM and Contact Angle Measurements

### 3.2.1 AFM and Contact Angle Measurements of Epindolidione films with Suberate and RC modification

The surface morphology studies before and after the functionalization of epindolidione surface with suberate and RC were conducted by using the AFM and contact angle techniques.

Fig. 20 shows the AFM images of the hydrogen-bonded organic semiconductor evaporated on silanized glass substrates. Crystal sizes of pristine epindolidione were found to be 60-80 nm in width and more than 300 nm in length. The well-organized epindolidione aggregates, which are responsible for the semiconducting properties, remain undisturbed through an overnight treatment with suberate solution (Fig. 20b) as well as through the RC incubation (Fig. 20c). Some changes in the roughness of the semiconductor are compared in Table 2 while surface functionalization.

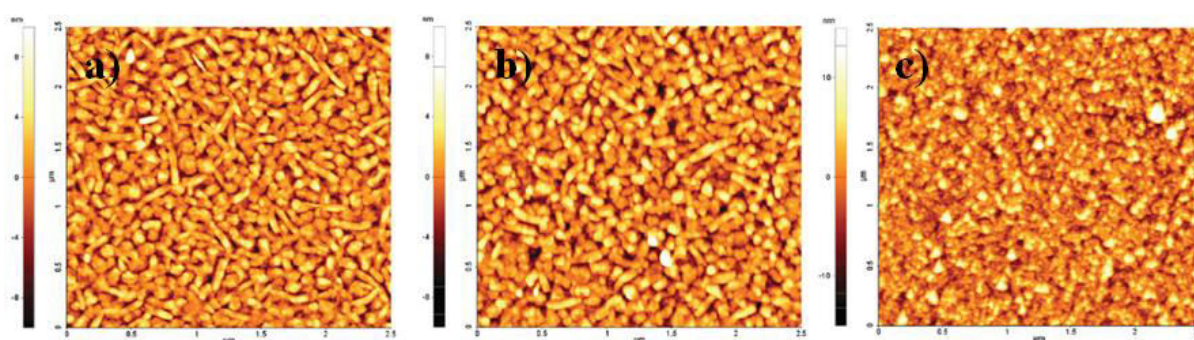


**Fig. 20:** AFM images of (a) pristine epindolidione, (b) epindolidione incubated with suberate, and (c) RC on suberate functionalized epindolidione after rinsing with PBS buffer solution

**Table 2:** Roughness and contact angle investigations on epindolidione films during suberate and RC functionalization

	<b>Unfunctionalized EPI</b>	<b>EPI with SUB</b>	<b>EPI with SUB and RC</b>
<b>Roughness [nm]</b>	2.9 ± 0.3	2.8 ± 0.5	4.6 ± 0.7
<b>Contact angle [°]</b>	86	74	<10

In addition, water contact angle measurements were carried out on the evaporated epindolidione films, from which the results are listed in Table 3. It is clearly shown that the surface properties of the hydrogen-bonded organic semiconductor pigment change after every incubation step. The untreated epindolidione has a more hydrophobic surface (86°), while incubation with suberate and RC afterwards the surface properties turn to be more and more hydrophilic (74° and <10, respectively).

All these results together indicate that the aliphatic suberate linker densely covers the surface of epindolidione, making a covalent bond with the lone pair of the amide group of the semiconductor and depositing hydrophilic *N*-succinimidyl leaving groups on the surface.

### 3.2.2 AFM and Contact Angle Measurements of Epindolidione films with Biotin and Streptavidin modification

Likewise, the same techniques were applied for the investigation of the surface modification on epindolidione with biotin and streptavidin.

Fig. 21 shows the AFM images of epindolidione films treated with biotin and streptavidin, respectively. The same morphological changes in the roughness, as in the suberate case, were obtained during the biotin functionalization as well.

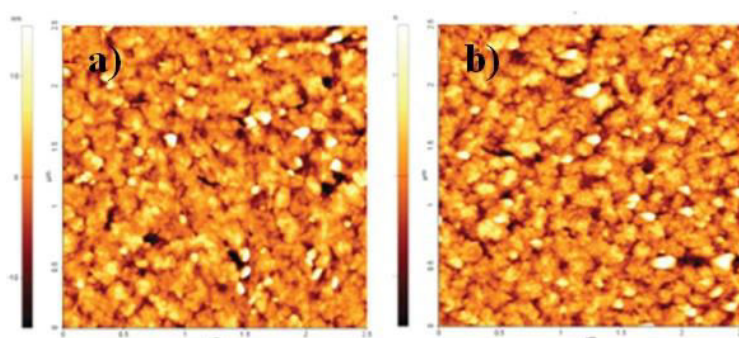


**Fig. 21:** Surface treatment of epindolidione films, (a) incubated with Biotin, (b) biotin-functionalized epindolidione surface incubated with streptavidin

Additionally, the contact angle determinations before and after incubation with biotin and streptavidin are a distinctive evidence for the surface modification of the epindolidione films and are consistent with the previous results as in the suberate case. Both, the roughness and contact angle results, are listed in Table 3.

**Table 3:** Roughness and contact angle investigations on epindolidione films during biotin and streptavidin functionalization

	<b>Unfunctionalized EPI</b>	<b>EPI with Biotin</b>	<b>EPI with Biotin and Streptavidin</b>
<b>Roughness [nm]</b>	2.9 ± 0.3	4.4 ± 0.4	4.8 ± 0.4
<b>Contact angle [°]</b>	86	71	<10

Since streptavidin is a much smaller protein than RC, no prodigious changes in morphology after incubation with the protein were recorded, however it is known that streptavidin can build aggregates of 100 nm size when deposited on flat surfaces [32]. In our case only approximately 30 nm of globular structures were found on epindolidione surface, which is not detected on the unfunctionalized epindolidione films. Fig. 22 shows streptavidin bioconjugated on the epindolidione with the corresponding height profile, evidencing the presence of small aggregates on the surface.

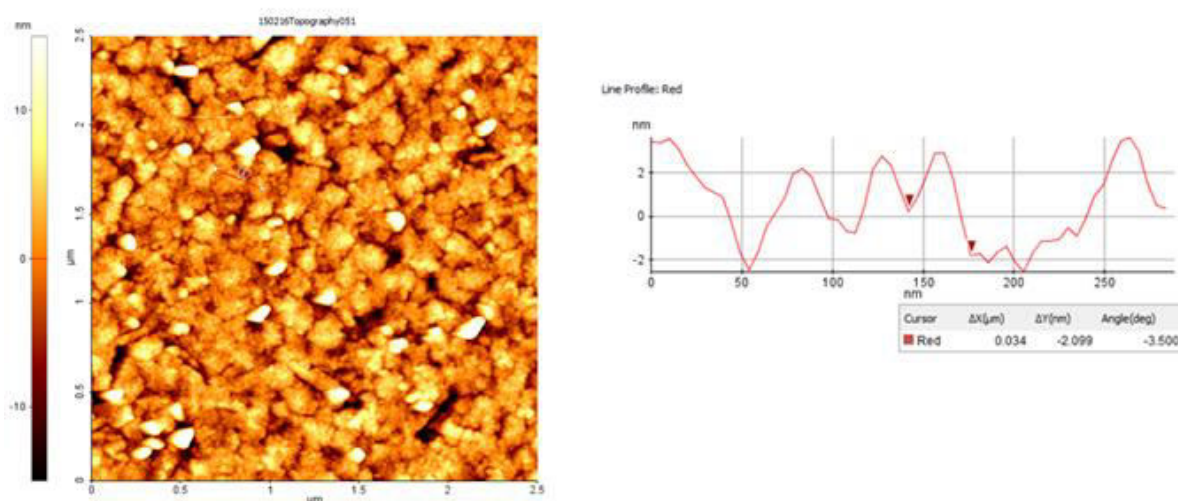


**Fig. 22:** Epindolidione film incubated with streptavidin and the corresponding height profile.

Based on the OFET discussions in the next chapters, we can declare that the biotinylation followed by a conjugation of streptavidin on the semiconductor occurs, however not necessarily as stable as expected.

### 3.3 OFET characterization

#### 3.3.1 Stability of Epindolidione OFETs

One of the motivations behind, using the hydrogen-bonded organic semiconductor pigment epindolidione in biosensing application is its stability both in air and aqueous environment. From our previously published work we know that the OFETs made out of epindolidione remain operational in harsh pH conditions from 3-10. Fig. 23 presents the low- voltage working epindolidione OFETs in different pH conditions over 360 cycles [16].

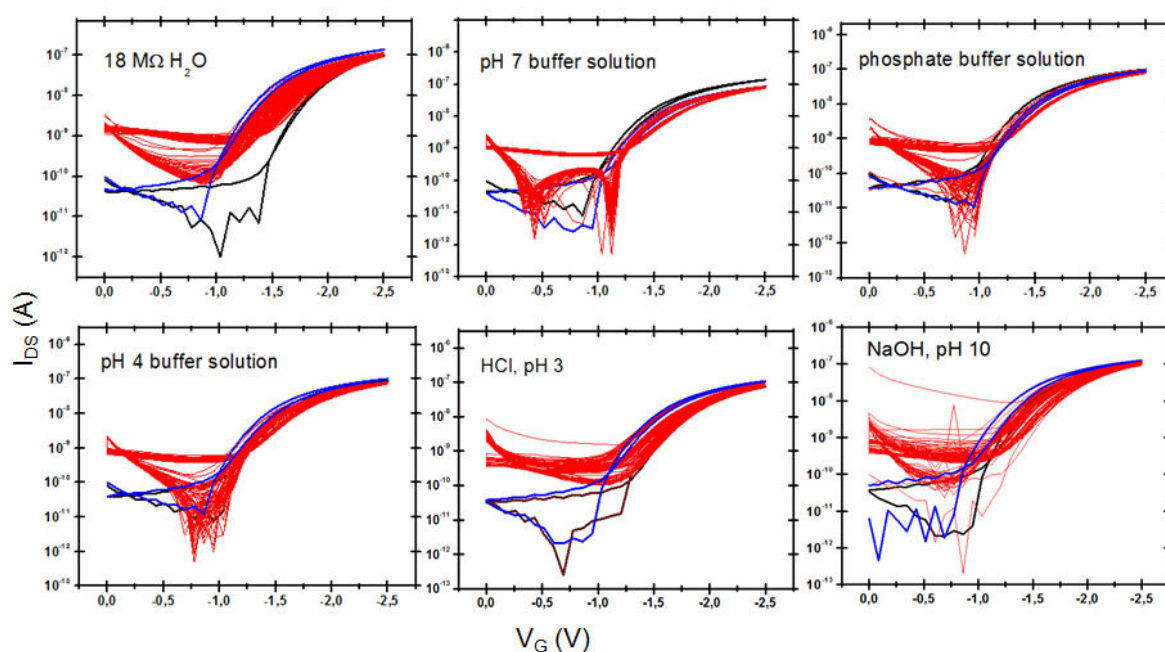


**Fig. 23:** Epi OFETs measured in air (black curves), 60 cycles in each electrolyte solution (red curves) and nominally dry after cycled measurements (blue curves).  $V_{ds}$  of  $-0.5V$  was applied. Devices were rinsed with deionized water between every electrolyte.

To operate the transistors in wet environment, high capacitance gate dielectrics was used in bottom-gate/top contact OFET configuration with epindolidione as the semiconductor and gold source-drain electrodes, respectively. The devices were measured dry in air and afterwards in different electrolyte solutions at different pH. A scan rate of  $150 \text{ mV s}^{-1}$ ,  $V_{ds}$  of  $-0.5 \text{ V}$  and  $V_g$  of  $-3V$  were selected in order to avoid any electrochemical reactions at the electrodes in the electrolyte solutions. Organic field-effect transistors, which were measured

in the dry state in air, show a saturation current of about 100 nA at  $V_g = -3V$  with an ON/OFF ratio of  $\sim 10^3$ . Afterwards, approximately 40  $\mu\text{L}$  of different electrolyte solutions are applied onto the device and measured 60 cycles for each step. The devices were rinsed with deionized water between every measurement. In every wet environment it was found that the OFF current is about 10 times higher than in the dry state, which is related to some dielectric screening effects. The OFF current is found to depend on the dielectric constant of the liquid with  $\sigma \propto \epsilon^{\frac{1}{2}}$ . This is interpreted in terms of an intercrystallite hopping model [17].

Furthermore, since the OFF current does not exceed  $\sim 1$  nA and is independent of the pH, we can say that a doping effect of the epindolidione layer can be excluded. After every pH measurement the ON current increased further and further, while the threshold voltage decreased. In Fig. 24 and 25 the transfer characteristics of OFETs are summarized in both acidic and alkaline directions. The transfer curves were recorded in nominally dry state after every electrolyte solution at different pH, measured over tens of cycles.

According to our knowledge usable OFETs were demonstrated at pH 7 in water [5], however no study has shown a stability of transistors in this large pH range. For this reason, having operational OFETs in these pH conditions, epindolidione is a highly interesting material for bioelectronic applications [16].

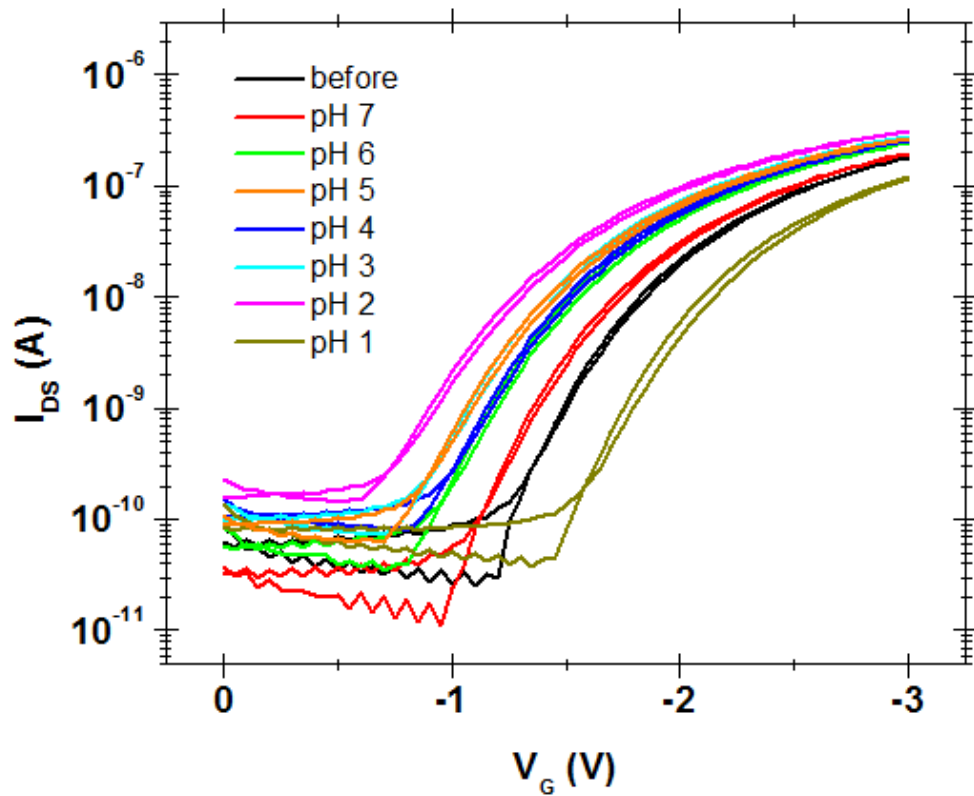


Fig. 24: Low-voltage EPI OFETs measured in air (black curve) and nominally dry after measured at different electrolytes in acidic pH 1-7, remaining stable over hundreds of cycles of measurements at  $V_{ds} = -0.5V$

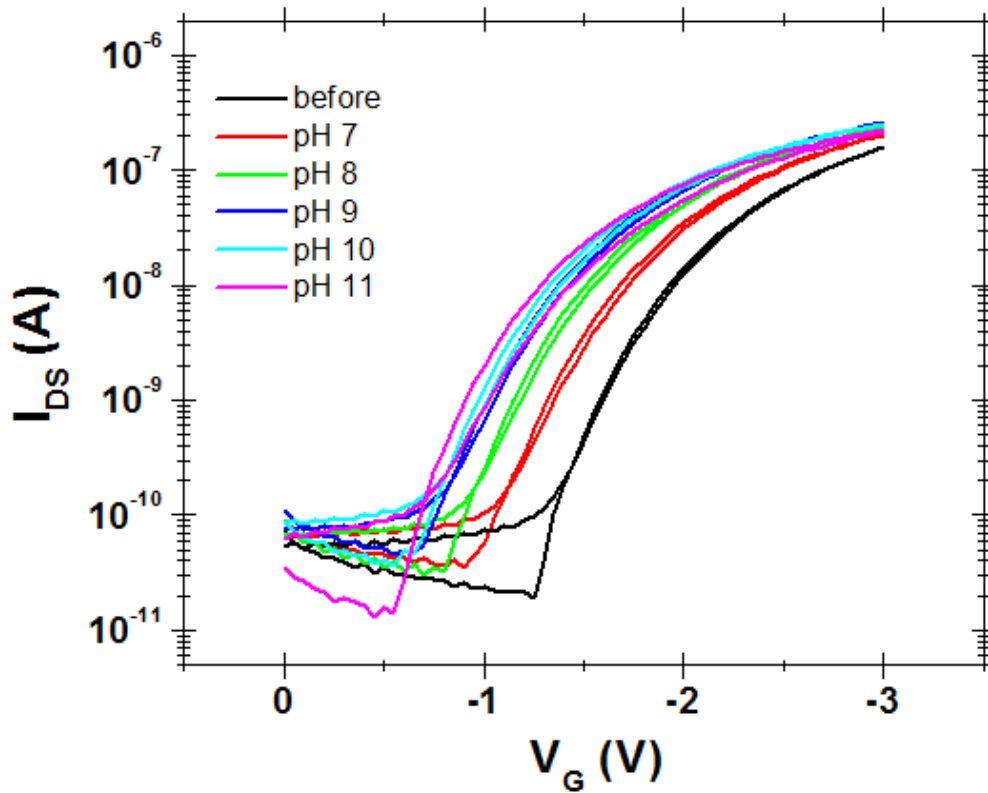


Fig. 25: Low-voltage EPI OFETs measured in air (black curve) and nominally dry after measured at different electrolytes in alkaline pH 7-11, remaining stable over hundreds of cycles of measurements at  $V_{ds} = -0.5V$

### 3.3.2 OFET response to Suberate and RC interaction on the Epindolidione surface

Since, according to the previous results, a surface functionalization of the hydrogen-bonded organic semiconductor epindolidione was achieved with different linkers and their respective protein pairs, we wanted to examine this bioconjugation in a working device.

As discussed in earlier chapters, OFETs are suitable candidates for biosensing applications due to their low-cost and simple processing, operation in wet environment, compatibility of flexible and large area substrates and consisting of highly chemically-tunable active layer materials [5,6]. Therefore bottom-gate/top-contact OFETs were fabricated with epindolidione as the semiconductor and gold as source-drain electrodes, respectively, both in direct contact with the aqueous medium without using any passivation method. In order to prevent any electrochemical reactions of the gold electrodes with the electrolyte solutions, the devices were operated in the linear regime at low  $V_{DS}$  (0.1-0.5 V) and  $V_G$  (3-3.5 V) values. The schematic of the device was already shown in Fig. 15.

Fig. 26 shows the transfer characteristics of the epindolidione OFETs before and after suberate functionalization. The OFETs were measured in the air in linear regime on nominally dry devices. After the suberate incubation on the epindolidione surface the mobility of the OFETs decreases from  $0.1 \text{ cm}^2 \text{ V}^{-1} \text{ s}^{-1}$  to  $0.06 \text{ cm}^2 \text{ V}^{-1} \text{ s}^{-1}$ , however the devices remain stable. By further RC incubation, however, OFETs start to degrade immediately, with no measurable modulation once incubated. This is most probably related to the presence of a highly polar LDAO surfactant in the RC solution, since test measurements with LDAO in water show an identical effect. Furthermore, it is obtained that the OFF current increases by about 100 pA while the threshold voltage decreases after functionalization [8].

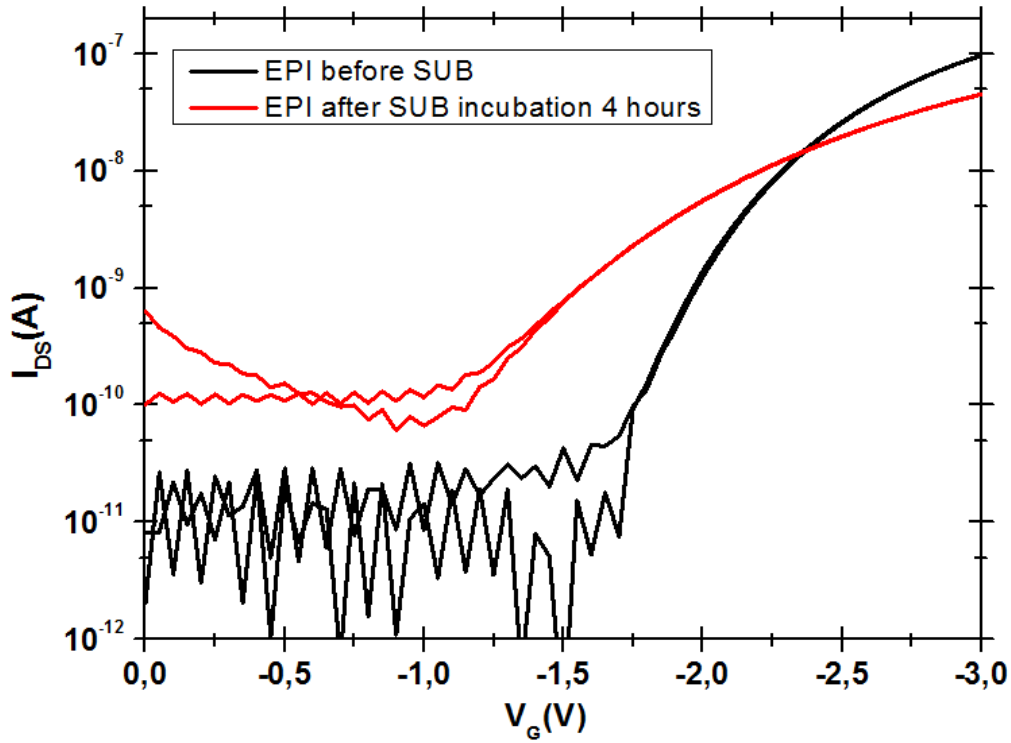
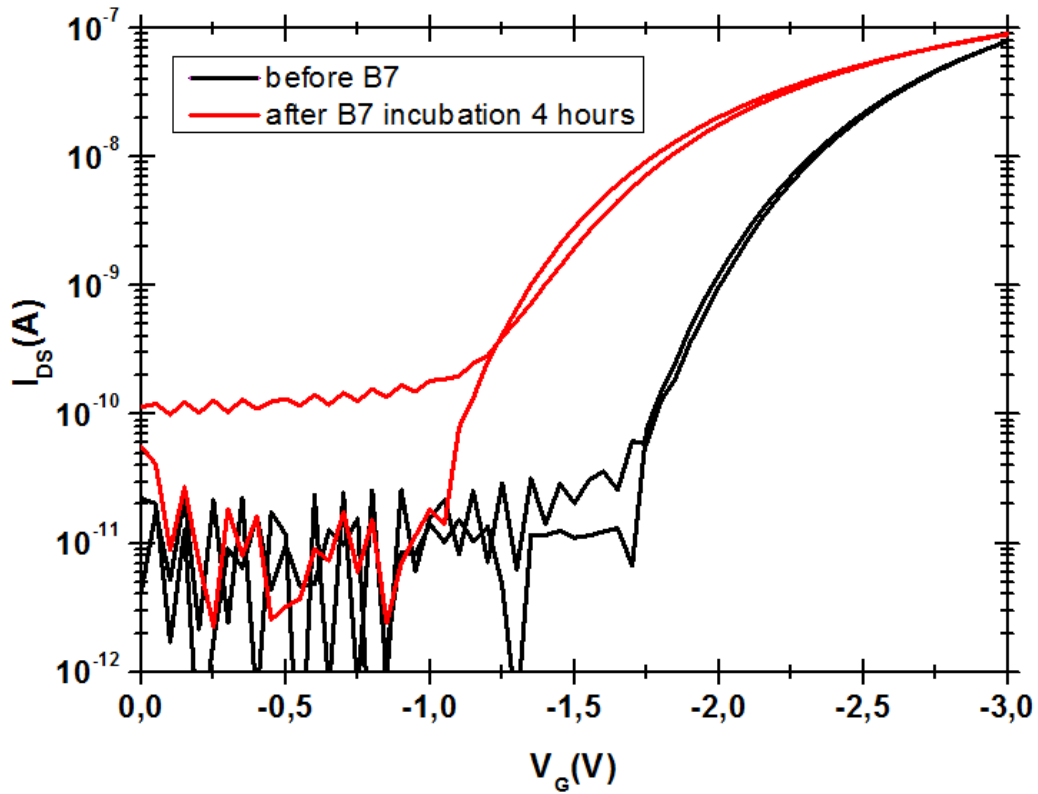


**Fig.26:** Linear-mode transfer curves of low-voltage epindolidione FETs before (black) and after (red) substrate incubation at  $V_{DS} = -0.5$  V

### 3.3.3 OFET response to Biotin and Streptavidin interaction on the Epindolidione surface

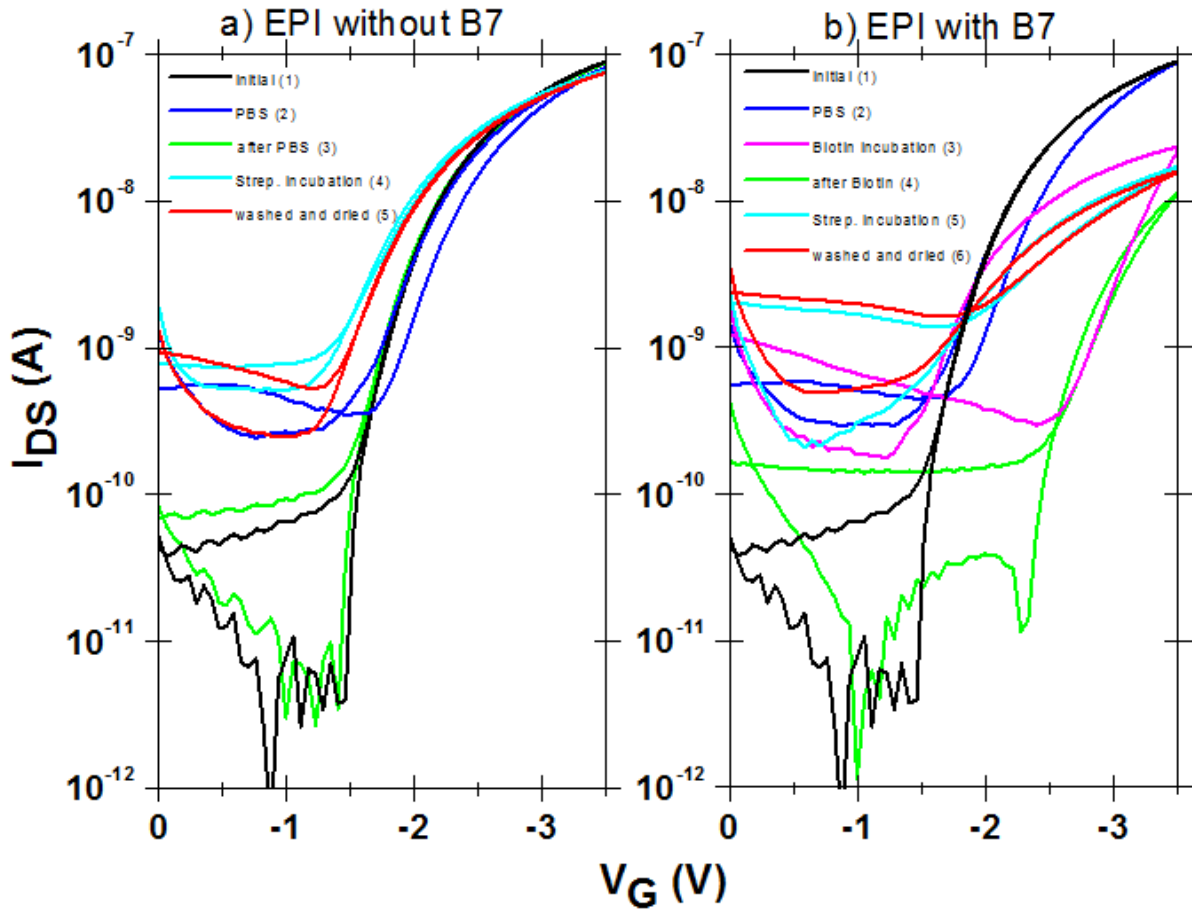
OFETs were fabricated, as discussed in chapter above, in order to test the biotin and streptavidin sensing on epindolidione surface.

Fig. 27 shows epindolidione FETs incubated with biotin for 4 hours. In comparison to the substrate case no change was obtained in the mobility of the device, however, the increase in the OFF current of about 100 pA and the decrease in the threshold voltage through biotin functionalization remained consistent.



**Fig.27:** Linear-mode transfer curves of low-voltage epindolidione FETs before (black) and after (red) biotin incubation at  $V_{DS} = -0.5$  V

A clear evidence for the bioconjugation of streptavidin was observed in the linear-mode epindolidione FETs. Biotin-functionalized devices show different responses to streptavidin in comparison to unfunctionalized ones, acting as control devices (Fig. 28). As shown in Fig. 28a, epindolidione FETs without biotin, exposed to the streptavidin solution, demonstrate a decrease of around 400 mV in threshold voltage relative to the same device measured in PBS, whereas the ON current remained unaffected. However, interestingly for the devices functionalized with biotin a decrease in the ON current occurred immediately when biotin incubation began, additionally with a pronounced hysteresis (Fig. 28b). By exposure of these devices to streptavidin, a drop in the threshold voltage of about 1 V and an increase in current were obtained. It was found that the threshold voltage is about 500 mV higher relative to unfunctionalized FETs incubated with streptavidin. Furthermore, this feature retained after washing the devices with PBS solution and drying.



**Fig.28:** Bioconjugation response to streptavidin of (a) unfunctionalized and (b) biotin-functionalized epindolidione FETs in comparison. Fig.28 (a) epindolidione devices measured in dry air at the beginning (black), in PBS solution (blue), after the measurement in PBS washed with water and dried (green), during streptavidin incubation in PBS (turquoise) and finally washed and dried (red). The same sequence of measurements was followed in Fig. 28 (b) with an additional incubation step with biotin (magenta). All measurements were conducted at  $V_{DS} = -0.5$  V.

Finally, it can be concluded that biotin modification can change the way epindolidione FETs respond to streptavidin. Furthermore we could detect some changes in the transfer characteristics of the OFETs after surface functionalization and found a platform, remaining operational before and after bioconjugation in aqueous environment indicating that epindolidione FETs are suitable applicants for next generation bioelectronics [16].

## 4 Conclusion

In this master thesis, the surface functionalization of the hydrogen-bonded organic semiconductor epindolidione with two aliphatic *N*-hydroxysuccinimide (NHS) functionalized linkers and two corresponding proteins was investigated. A straightforward bioconjugation protocol as well as a general binding mechanism were developed on the semiconductor surface.

Disuccinimidylsuberate and RC, and succinimidyl biotinate and streptavidin lock-and-key systems were investigated: both systems are well established in biotechnological applications. The bioconjugation of the semiconductor surface and the further detection of the proteins RC and streptavidin with their corresponding linkers were successfully achieved. AFM, contact angle, FTIR and OFETs were used for the surface verification.

The AFM and contact angle measurements were consistent for both biosystems regarding changes in the roughness of the semiconductor pigment and decrease of water contact angle on the epindolidione surface after functionalization.

The FTIR results show more enhanced bioconjugation evidence on epindolidione with suberate and RC with additional amide I and amide II peaks, indicating that the surface functionalization was attained. Furthermore, in order to test the type of binding during the bioconjugation, washing steps were performed on silanized ITO glass slides with epindolidione incubated with RC. It was found that on the epindolidione surface only with RC, the protein could be washed away, whereas on the epindolidione functionalized with suberate, RC signal remained even after washing with PBS.

Unfortunately, the same success was not exactly achieved with epindolidione and biotin bioconjugation system in FTIR spectra. Epindolidione surface once incubated with biotin showed indeed distinctive IR signals, however, after washing with PBS these peaks disappear. From the literature about biotin immobilization it has been suggested that the signals belonging to biotin disappear during aqueous washing procedure although the linker is still present. The reasons for this disappearance were explained as shielding or other changes in the environment effecting the vibrational properties of the ureido ring.

We succeeded in the bioconjugation of the hydrogen-bonded semiconductor pigment epindolidione via nucleophilic attack of the N-H group of epindolidione on the carbonyl group of the linker with having NHS as leaving groups on the surface. As mentioned above, the surface functionalization of the semiconductor was supported by morphology and spectroscopy studies. Next, we asked ourselves the question, if we can see any functionalization effect on an operational and applicable device. According to our previously published research we paid attention towards organic field-effect transistors. We have found that transistors made out of epindolidione remain operational in aqueous environments at harsh pH conditions from 3-10. So would it be possible to fabricate an epindolidione OFET, functionalize it on the device surface with aqueous linkers and proteins via simple processing and then finally detect those biomolecules? Would such a sensitive device survive these circumstances and would both the semiconducting properties of the pigment and the biological functionality of the proteins remain well preserved during operation? The results from this thesis indicate that these things are indeed possible.

Therefore bottom-gate/top-contact organic field-effect transistors made out of epindolidione were produced and operated in linear-mode at low-voltages in order to avoid any unexpected electrochemical reactions. Clear evidences for the appearance of the linkers on the semiconductor surface were obtained in transfer characteristics responses to different biomolecules.

For both linkers, it was obtained that the OFF current increased while the threshold voltage decreased after functionalization. Additionally, in the suberate case a decrease in the mobility from  $0.1 \text{ cm}^2 \text{ V}^{-1} \text{ s}^{-1}$  to  $0.06 \text{ cm}^2 \text{ V}^{-1} \text{ s}^{-1}$  was shown. However, by further RC incubation OFETs start to degrade immediately, with no measurable modulation once incubated. This is most probably related to the presence of a highly polar LDAO surfactant in the RC solution, since test measurements with LDAO in water show an identical effect. Different responses were obtained when the streptavidin response of biotin-functionalized versus unfunctionalized epindolidione FETs were evaluated. Epindolidione FETs without biotin, exposed to the streptavidin solution, demonstrate a decrease in threshold voltage relative to the same device measured in PBS, whereas the ON current remained unaffected. However, for the devices functionalized with biotin a decrease in the ON current occurred immediately when biotin incubation begun with a pronounced hysteresis. By exposure of these devices to streptavidin, a drop in the threshold voltage and an increase in current were obtained. It was found that the threshold voltage is higher relative to unfunctionalized FETs incubated with streptavidin.

Interestingly, this feature was retained after washing the devices with PBS solution and drying. All this experimental evidence suggests that biotin modification changes the way epindolidione FETs respond to streptavidin.

We believe that with all these results together, we can conclude that the surface functionalization of the epindolidione pigment was achieved and supported with various kinds of experimental techniques. Hence, it is evident that the hydrogen-bonded organic semiconductor epindolidione and its aqueous-based surface functionalized FETs continue to be operational in "wet" environments and seem to be promising materials and platforms for biosensing applications in the future.

## 5 Literature

- [1] O. Knopfmacher, M. L. Hammock, A. L. Appleton, G. Schwartz, J. Mei, T. Lei, J. Pei, Z. Bao; Highly stable organic polymer field-effect transistor sensor for selective detection in the marine environment; *Nature Communications*; **2013**; 5.
- [2] R. M. Owens, G. G. Malliaras; Organic Electronics at the Interface with Biology; *MRS BULLETIN*; **2010**; 35; 449-456.
- [3] Images in Paediatric Cardiology; US National Library of Medicine; National Institutes of Health; <http://www.ncbi.nlm.nih.gov/pmc/articles/PMC3232561/>, [August 6<sup>th</sup>, 2015].
- [4] G. M. Walker, J. M. Ramsey, R. K. Cavin, D. J.C. Herr, C. I. Merzbacher, V. Zhirnov; A Framework for BIOELECTRONICS Discovery and Innovation; **2009**.
- [5] M. E. Roberts, S. C. B. Mannsfeld, N. Queraltó, C. Reese, J. Locklin, W. Knoll, Z. Bao; Water-stable organic transistors and their application in chemical and biological sensors; *PNAS*; **2008**; 105; 12134–12139.
- [6] H. U. Khan , M. E. Roberts , O. Johnson , R. Förch ,W. Knoll , Z. Bao; In Situ, Label-Free DNA Detection Using Organic Transistor Sensors; *Adv. Mater.*; **2010**; 22; 4452–4456.
- [7] L. Torsi, G. M. Farinola, F. Marinelli, M. C. Tanese, O. H. Omar, L. Valli, F. Babudri, F. Palmisano, P.G. Zambonin, F. Naso; A sensitivity-enhanced field-effect chiral sensor; *Nature Materials*; **2008**;7; 412-417.
- [8] R. R. Tangorra, H. Coskun, A. Antonucci, D. Farka, A. Operamolla, Y. Kanbur, F. Milano, M. Trotta, G. M. Farinola, E. D. Głowacki, N. S. Sariciftci; Bioconjugation of hydrogen-bonded organic semiconductors with functional proteins; *J. Mat. Chem. C*; **2015**; 3; 6554-6564.
- [9] F. Milano, R. R. Tangorra, O. H. Omar, R. Ragni, A. Operamolla, A. Agostiano, G. M. Farinola, M. Trotta, Enhancing the light harvesting capability of a photosynthetic reaction center by a tailored molecular fluorophore; *Angew. Chem. Int. Ed.*, **2012**, 51, 11019–23.
- [10] Thermo Fischer Scientific; <https://www.lifetechnologies.com/at/en/home/life-science/protein-biology/protein-biology-learning-center/protein-biology-resource-library/pierce-protein-methods/avidin-biotin-interaction.html>; [August 10<sup>th</sup>, 2015].

- [11] Protein Data Bank Europe:  
<http://www.ebi.ac.uk/pdbe/widgets/QuipStories/avidin/avidin.pdf> [August 10<sup>th</sup>, 2015].
- [12] L. Chalet, P. J. Wolf; The Properties of Streptavidin, a Biotin-Binding Protein Produced by Streptomyces; *Archives of biochemistry and biophysics*; **1964**; *106*; 1-5.
- [13] E. D. Głowacki , M. I. Vladu , M. Kaltenbrunner , J. Gasiorowski , M. S. White , U. Monkowius , G. Romanazzi , G. P. Suranna , P. Mastrorilli , T. Sekitani , S. Bauer , T. Someya , L. Torsi , N. S. Sariciftci; Hydrogen-Bonded Semiconducting Pigments for Air-Stable Field-Effect Transistors; *Adv. Mater.*; **2013**; *25*; 1563–1569.
- [14] E. D. Głowacki; Hydrogen-bonded pigments for organic electronic applications; Dissertation, JKU, **2013**.
- [15] E. D. Głowacki, M. I. Vladu , S. Bauer, N. S. Sariciftci; Hydrogen-bonds in molecular solids – from biological systems to organic electronics; *J. Mater. Chem. B*; **2013**; *1*; 3742-3753.
- [16] E. D. Głowacki, G. Romanazzi , C. Yumusak , H. Coskun , U. Monkowius , G. Voss , M. Burian , R. T. Lechner , N. Demitri , G. J. Redhammer , N. Sünger , G. P. Suranna, N. S. Sariciftci, Epindolidiones—Versatile and Stable Hydrogen-Bonded Pigments for Organic Field-Effect Transistors and Light-Emitting Diodes; *Adv. Funct. Mater.*; **2014**.
- [17] H. Coskun, Y. Kanbur, C. Yumusak, E. D. Głowacki, N. S. Sariciftci; Hydrogen-bonded pigments for transistors with stable operation directly in contact with aqueous electrolytes of pH 1-10; in preparation.
- [18] B. Cappella, G. Dietler; Force-distance curves by atomic force microscopy; *Surface Science Reports*; **1999**; *34*; 1-104.
- [19] G. Binnig, C. F. Quate, Ch. Gerber; Atomic Force Microscope; *PHYSICAL REVIEW LETTERS*; **1986**; *56*.
- [20] Atomic force microscopy (AFM), <http://perso.univ-lemans.fr/~bardeau/IMMM-PEC/afm/afmintroduction.html>; [August 15<sup>th</sup>, 2015].
- [21] Research on biological atomic force microscopy, <http://web.physics.ucsb.edu/~hhansma/biomolecules.htm>; [August 15<sup>th</sup>, 2015].

- [22] Ramehart; Information on contact angle, <http://www.ramehart.com/contactangle.htm>; [September 2<sup>nd</sup>, 2015].
- [23] Biolin Scientific, Process together, <http://www.biolinscientific.com/attension/applications/?card=AA7>; [September 2<sup>nd</sup>, 2015].
- [24] M. Mas- Torrent and C. Rovira; Role of Molecular Order and Solid-State Structure in Organic Field-Effect Transistors; *Chem. Rev.*; **2011**; *111*; 4833-4856.
- [25] C. Di, F. Zhang, D. Zhu; Multi-Functional Integration of Organic Field-Effect Transistors (OFETs): Advances and Perspectives; *Adv. Mater.*; **2013**, *25*, 313-330.
- [26] S. Schaur; Electrochemical doping of organic field- effect transistors to improve contact resistances; Diploma thesis; **2010**.
- [27] N. Marjanović; Photoresponsive Organic Field-Effect Transistors using Organic Semiconductors and Dielectrics; PhD. Thesis, **2005**.
- [28] P. Stadler; Hysterisis in Bio- organic field effect transistors; Diploma thesis, **2006**.
- [29] A.I. Mardare, M. Kaltenbrunner, N.S. Sariciftci, S. Bauer and A.W. Hassel, Ultra-thin anodic alumina capacitor films for plastic electronics, *Phys.Status Solidi A*, **2012**, *209*, 813-818.
- [30] Biointerface Characterization by Advanced IR Spectroscopy, ed. C.M. Pradier and Y.J. Chabel, Elsevier, Amsterdam, 1st edn, **2011**.
- [31] Functionalization of Semiconductor Surfaces, ed. F. Tao and S.L. Bernasek, Wiley, Hoboken, **2012**.
- [32] M. D. Angionea, S. Cotronea, M. Magliuloa, A. Mallardib, D. Altamura, C. Gianninic, N. Cioffia, L. Sabbatinia, E. Fratinid, P. Baglionid, G. Scamarcioe, G. Palazzoa, L. Torsia; Interfacial electronic effects in functional bilayers integrated into organic field-effect transistors; *PNAS*; **2012**; *109*; 6429–6434.

## 6 Curriculum Vitae

### PERSONAL INFORMATION

---

<b>Name</b>	Halime Coskun
<b>Date of Birth</b>	May 11, 1991
<b>Birth Place</b>	Linz, Austria
<b>Nationality</b>	Turkey
<b>Contact Address</b>	Altenbergerstr. 69, 4040 Linz, Austria

### ACADEMIC QUALIFICATIONS

---

<b>Oct 2013-</b>	<b>Degree-Diplom-Ingenieurin :</b> Johannes Kepler University , Faculty of Natural Science , Technical Chemistry, Linz, Austria
<b>Oct 2010 –Jun 2013</b>	<b>Degree- BSc :</b> Johannes Kepler University , Faculty of Natural Science , Technical Chemistry, Linz, Austria
<b>Sep2002 – May 2005</b>	<b>HSC/ Science :</b> Bundesrealgymnasium, Landwiedstr. 82, 4020 Linz

### RESEARCH EXPERIENCE

---

<b>Jul 2010</b>	<b>Medical Internship</b> Dr. Andrea Gussner-Langl
<b>Aug 2011</b>	<b>Pharmaceutical Internship</b> Mag. pharm. Julia Rothenthal
<b>Feb -Aug 2013</b>	<b>Bachelor student at Johannes Kepler University</b> LIOS, Linz Institute for Organic Solar Cells, Physical Chemistry
<b>Oct 2013- Sept 2015</b>	<b>Master student at Johannes Kepler University</b> LIOS, Linz Institute for Organic Solar Cells, Physical Chemistry

## RESEACH ACTIVITIES

---

### Conferences/Workshops Attended

Solar Energy for World Peace, 2013

BioEL- International Winterschool on Bioelectronics, 2014

IWOBOE- International Workshop on Flexible Bio-and Organic Printed Electronics, 2014

BioEL- International Winterschool on Bioelectronics, 2015

E-MRS, European Materials Research Society, 2015

### Research Publications

1. Hydrogen-bonded diketopyrrolopyrrole (DPP) pigments as organic semiconductors, *Organic Electronics*, **2014**, *15*, 3521-3528.
2. Epindolidiones- Versatile and Stable Hydrogen-Bonded Pigments for Organic Field-Effect Transistors and Light-Emitting Diodes, *Adv. Func. Mat.*, **2015**, *25*, 5.
3. Bioconjugation of hydrogen-bonded organic semiconductor with functional proteins, *J.Mater. Chem. C*, **2015**, *3*, 6554.
4. Hydrogen-bonded pigments for transistors with stable operation directly in contact with aqueous electrolytes of pH 1-10; in preparation.